Liquid Crystals
Publication details, including instructions for authors and subscription information:
http://www.informaworld.com/smpp/title~content=t713926090

Heterocyclic polycatenar liquid crystals

Catherine Fang He[a]; Gary J. Richards[a]; Stephen M. Kelly[a]; Adam E. A. Contoret[b]; Mary O'neill[b]
[a] Department of Chemistry, University of Hull, Hull, HU6 7RX, UK [b] Department of Physics, University of Hull, Hull, HU6 7RX, UK

To cite this Article He, Catherine Fang , Richards, Gary J. , Kelly, Stephen M. , Contoret, Adam E. A. and O'neill, Mary(2007) 'Heterocyclic polycatenar liquid crystals', Liquid Crystals, 34: 11, 1249 — 1267
To link to this Article: DOI: 10.1080/02678290701682373
URL: http://dx.doi.org/10.1080/02678290701682373

Liquid Crystals, Vol. 34, No. 11, November 2007, 1249–1267

Taylor & Francis
Taylor & Francis Group

Heterocyclic polycatenar liquid crystals

CATHERINE FANG HE†, GARY J. RICHARDS†, STEPHEN M. KELLY†*, ADAM E. A. CONTORET‡ and MARY O'NEILL‡

†Department of Chemistry, University of Hull, Cottingham Road, Hull, HU6 7RX, UK
‡Department of Physics, University of Hull, Cottingham Road, Hull, HU6 7RX, UK

(*Received 24 May 2007; accepted in final form 30 August 2007*)

We report the synthesis of polycatenar liquid crystals incorporating 2,5-disubstituted [1, 3, 4]-oxadiazole and [1, 3, 4]-thiadiazole rings joined by a combination of carbon–carbon single and double bonds (–CH=CH–). The ratio of the aromatic core to the aliphatic chains was varied systematically by changing the number of the aliphatic chains, from two to six, and their length, from short to very long, i.e. from methoxy to hexadecyloxy. The shape anisotropy of the core was varied by exchanging the oxygen atom in the [1, 3, 4]-oxadiazole for a sulfur atom to form the corresponding [1, 3, 4]-thiadiazole ring with a smaller deviation from coaxiality of the bonds in the 2,5-positions. The shape anisotropy of the core was increased by the presence of an additional phenylenevinylene unit in a series of tetracatenar oxadiazoles. We report the synthesis, physical properties and polymerization of a polycatenar reactive mesogen in a columnar phase to form a polycatenar polymer network.

1. Introduction

Liquid crystals may have significant potential as organic semiconductors in a range of plastic electronics, such as organic field-effect transistors (OFETs), organic light-emitting diodes (OLEDs) and photovoltaics [1]. Columnar (discotic) liquid crystals, such as triphenylenes [2–5] and phthalocyanines [6–8], have been reported to exhibit large charge carrier mobility [2–10]. The charge carrier mobility ($10^{-1}\,cm^2\,V^{-1}\,s^{-1} > \mu_h > 10^{-3}\,cm^2\,V^{-1}\,s^{-1}$) observed for the ordered hexagonal columnar phase of hexakis(*n*-alkoxy)triphenylenes and the helical columnar phase of the hexakis(*n*-alkylthio)triphenylenes [4] are intermediate between those observed for organic single crystals and inorganic semiconductors ($\mu \geqslant 1\,cm^2\,V^{-1}\,s^{-1}$) and those ($10^{-3}\,cm^2\,V^{-1}\,s^{-1} > \mu > 10^{-6}\,cm^2\,V^{-1}\,s^{-1}$) of amorphous conjugated polymers. Columnar liquid crystals generally consist of disc-shaped molecules or self-assembled aggregates organised in a supramolecular structure of nearly parallel columns of varying degrees of order in a two-dimensional lattice [6–12]. Holes, rather than electrons, are the majority charge carriers due to the limited electron affinity and low ionization potential of the electron-rich aromatic cores of columnar liquid crystals incorporating many phenyl rings. The charge transport is non-dispersive and the charge carrier mobility parallel to the director (parallel to the core of the columns of self-assembled disks) is orders of magnitude higher than that measured orthogonal to the director, i.e. between columns. This anisotropy of transport is attributable, at least in part, to the insulating nature of the lateral aliphatic chains surrounding the aromatic cores.

In order for columnar (discotic) liquid crystals with an aromatic central core to be useful as organic semiconductors, the columnar phase must be aligned uniformly and macroscopically with the columns orthogonal or parallel to the substrate surface. Columnar liquid crystals with large polyaromatic cores, such as coronenes, exhibit the largest values for charge carrier mobility ($\mu \approx 4 \times 10^{-1}\,cm^2\,V^{-1}\,s^{-1}$) so far [11, 12]. Unfortunately, the very high clearing point of such columnar liquid crystals renders them very difficult to align by cooling from the isotropic liquid into the column phase followed by annealing in the columnar state. Polycatenar compounds, with more than one terminal chain at each end of a rod-like molecule, can also exhibit columnar phases, although they possess a linear molecular structure [13–17]. Three or four linear molecules can self-assemble and aggregate to form disks, which then form stacks of disks one on top of the other in to a fluid macroscopic columnar structure. Therefore, the calamitic and columnar mesophases of polycatenar liquid crystals may be of interest as organic semiconductors with charge-transporting

*Corresponding author. Email: S.M.Kelly@hull.ac.uk

Liquid Crystals
ISSN 0267-8292 print/ISSN 1366-5855 online © 2007 Taylor & Francis
http://www.tandf.co.uk/journals
DOI: 10.1080/02678290701682373

and/or electroluminescent properties for applications in plastic electronics [1, 18–22]. A range of small molecules, oligomers, dendrimers and polymers incorporating the 2,5-disubstituted [1, 3, 4]-oxadiazole moiety, often with phenyl rings in the 2- and 5-positions, has been synthesised for use as electron-transport layers as in OLEDs [23, 24]. We now report a systematic study of polycatenar liquid crystals incorporating the 2,5-disubstituted [1, 3, 4]-oxadiazole and [1, 3, 4]-thiadiazole rings joined by a combination of carbon–carbon single and double bonds (–CH=CH–) as potential organic semiconductors. The planar, conjugated nature of the phenylenevinylene unit has been shown to be a suitable component of the aromatic core of luminescent hexacatenars with columnar phases [20–22].

An initial problem associated with the practical fabrication of multilayer OLEDs with low-molar-mass liquid crystals forming charge-transport layer was the fluid nature of the liquid crystalline state. This could have resulted in interlayer mixing during the deposition of subsequent layers by vapour deposition or spincoating [1]. This problem was resolved by photochemically polymerizing liquid crystalline monomers with two polymerizable groups on the end of the aliphatic chains attached to the cores of the molecules (reactive mesogens) to form insoluble and intractable crosslinked polymer networks with liquid crystalline and organic semiconductor properties [1, 25–36]. These reactive mesogens are photopatternable. So far nematic, smectic and discotic reactive mesogens have been converted into polymer networks for semiconductor applications [1]. We now report the synthesis of a polycatenar reactive mesogen and its polymerization to form an insoluble polymer network.

2. Experimental

2.1. *Instrumentation*

All commercially available starting materials, reagents and solvents were used as supplied (unless otherwise stated) and were obtained from Aldrich, Strem Chem. Inc, Acros or Lancaster Synthesis. All reactions were carried out using a dry nitrogen atmosphere unless water was present as solvent or reagent and the temperatures were measured internally. Mass spectra were recorded using a gas chromatography/mass spectrometer (GC/MS)-QP5050A Schimadzu with electron impact (EI) at a source temperature of 200°C. Compounds with an RMM $>800\,g\,mol^{-1}$ were analysed using a Bruker, reflex IV, matrix-assisted laser desorption/ionization (MALDI), time of flight (TOF) MS. A 384 well microlitre plate format was used with a scout target. Samples were dissolved in DCM with HABA (2-(4-hydroxyphenylazo)benzoic acid) matrix (1:10, respectively). The mass ion of the material is identified by M^+. ^1H NMR spectra were recorded using a JEOL Lambda 400 spectrometer and an internal standard of tetramethylsilane (TMS) was used. GC was carried out using a Chromopack CP3800 gas chromatograph equipped with a 10 m CP-SIL 5CB column. Purification of intermediates and final products was mainly accomplished by gravity column chromatography, using silica gel (40–63 μm, 60 A) obtained from Fluorochem. The purity of the final compounds was determined by elemental analysis using a Fisons EA 1108 CHN analyser. The melting point and the other transition temperatures of the solid compounds prepared were measured using a Linkam 350 hot-stage and control unit in conjunction with a Nikon E400 polarising microscope. The liquid crystal transition temperatures of all of the final products were confirmed using a Perkin-Elmer DSC-7 and in conjunction with a TAC 7/3 instrument controller, using the peak measurement for the reported value of the transition temperatures. The photopolymerization of the reactive mesogen was carried out using standard procedures [34–36]. The absorption and emission spectra as well as FTIR were also measured using standard methods [34–36].

2.2. *Synthesis*

The polycatenar oxadiazoles (**8**; R_1, R_2, R_3=H and $C_nH_{2n+1}O$) and thiadiazoles (**9**; R_1, R_2, R_3=H and $C_nH_{2n+1}O$) were prepared as shown in reaction scheme 1. Commercially available 4-iodobenzoic acid (**1**) was converted into the corresponding acid chloride (**2**) using oxalyl chloride or thionyl chloride, which was reacted with hydrazine hydrate to form the symmetrical diamide (**3**). This diketone is then converted to the intermediate bis(4-iodophenyl)-1,3,4-oxadiazole (**4**; X=O) using phosphorous pentoxide [37] and the intermediate bis(4-iodophenyl)-1,3,4-thiadiazole (**4**; X=S) using P_4S_{10} [38]. A Heck reaction [39] between the alkoxy-substitued styrenes (**7**; R_1, R_2, R_3=H and $C_nH_{2n+1}O$) and the bis(4-iodophenyl)-1,3,4-oxadiazole (**4**; X=O) yielded the bicatenar oxadiazoles (**8**; R_1, R_2, R_3=H and $C_nH_{2n+1}O$). An analogous Heck reaction between bis(4-iodophenyl)-1,3,4-thiadiazole (**4**; X=S) gave the polycatenar thiadiazoles (**9**; R_1, R_2, R_3=H and $C_nH_{2n+1}O$). The alkoxy-substituted styrenes (**7**; R_1, R_2, R_3=H and $C_nH_{2n+1}O$) were prepared in a Wittig reaction [40] using a methyltriphenylphosphonium salt from the appropriate alkoxy-substituted benzaldehydes (**6**; R_1, R_2, R_3=H and $C_nH_{2n+1}O$), prepared by the usual Williamson alkylation [41] of commercially available hydroxy-substituted benzaldehydes (**5**; R_1, R_2, R_3=H and HO).

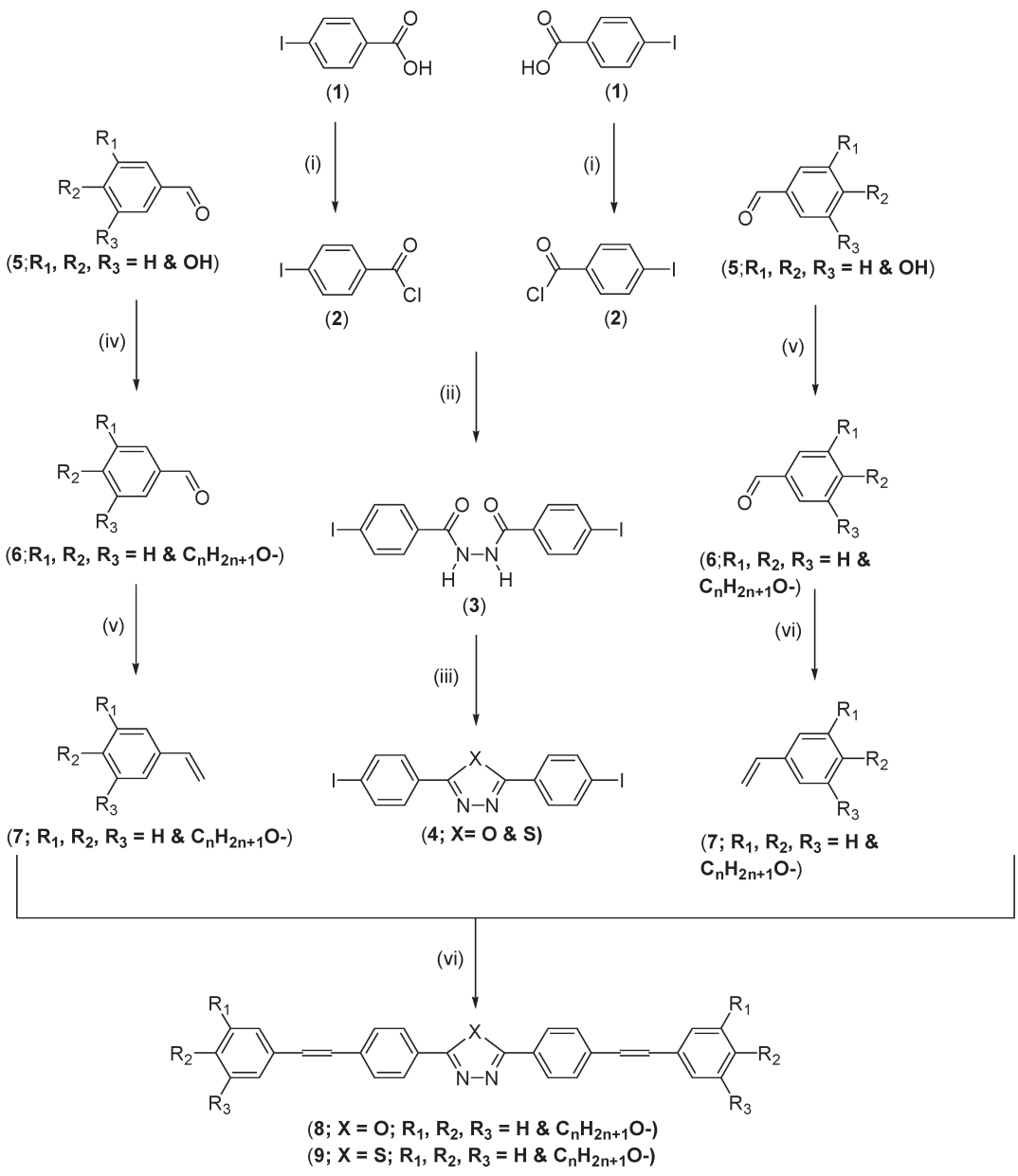

Scheme 1. Reagents and conditions: (i) $(COCl)_2$, DMF, CH_2Cl_2; (ii) $H_2N.NH_2$, THF, pyridine; (iii) $POCl_3$ (X=O) or P_4S_{10}, (X=S) pyridine; (iv) $C_nH_{2n+1}Br$, K_2CO_3, $C_2H_5COCH_3$; (v) $CH_3P(C_6H_5)_3Br$, $KOC(CH_3)_3$, DME; (vi) $(CH_3CO_2)_2Pd$, $P(\sigma\text{-}CH_3C_6H_5)_3$, DMF, $N(C_2H_5)_3$.

The longer tetracatenar 2,5-bis{4-[(*E*)-2-(3,4-dialkoxystyrene)styryl]phenyl}-[1, 3, 4]-oxadiazoles (**13**) were synthesised as shown in reaction scheme 2. The alkoxy-substituted styrenes (**7**; $R_1=R_2=C_nH_{2n+1}O$; $R_3=H$) were reacted with 4-bromobenzaldehyde (**10**) in a Heck reaction [39, 40] to yield the 4-(3,4-dialkoxystyryl)benzaldehydes (**11**), which were converted in a Wittig reaction [40] using a methyltriphenylphosphonium salt into the corresponding 4-(3,4-dialkoxystyryl)styrenes (**12**). Another Heck reaction between the 4-(3,4-dialkoxystyryl)styrenes (**12**) and bis (4-iodophenyl)-1,3,4-oxadiazole (**4**; X=O) yielded the desired tetracatenar oxadiazoles (**13**). Herrman's catalyst, *trans*-di-μ-acetatobis[2-(di-*o*-tolylphosphino)benzyl] dipalladium(II), was used sometimes since it has been reported to be the most active catalysts for the Heck coupling of aryl halides with olefins [42].

The reactive mesogen (**19**) was synthesised analogously, as shown in reaction scheme 3. The 3,4-dihydroxybenzaldehyde (**5**) was alkylated as usual in a

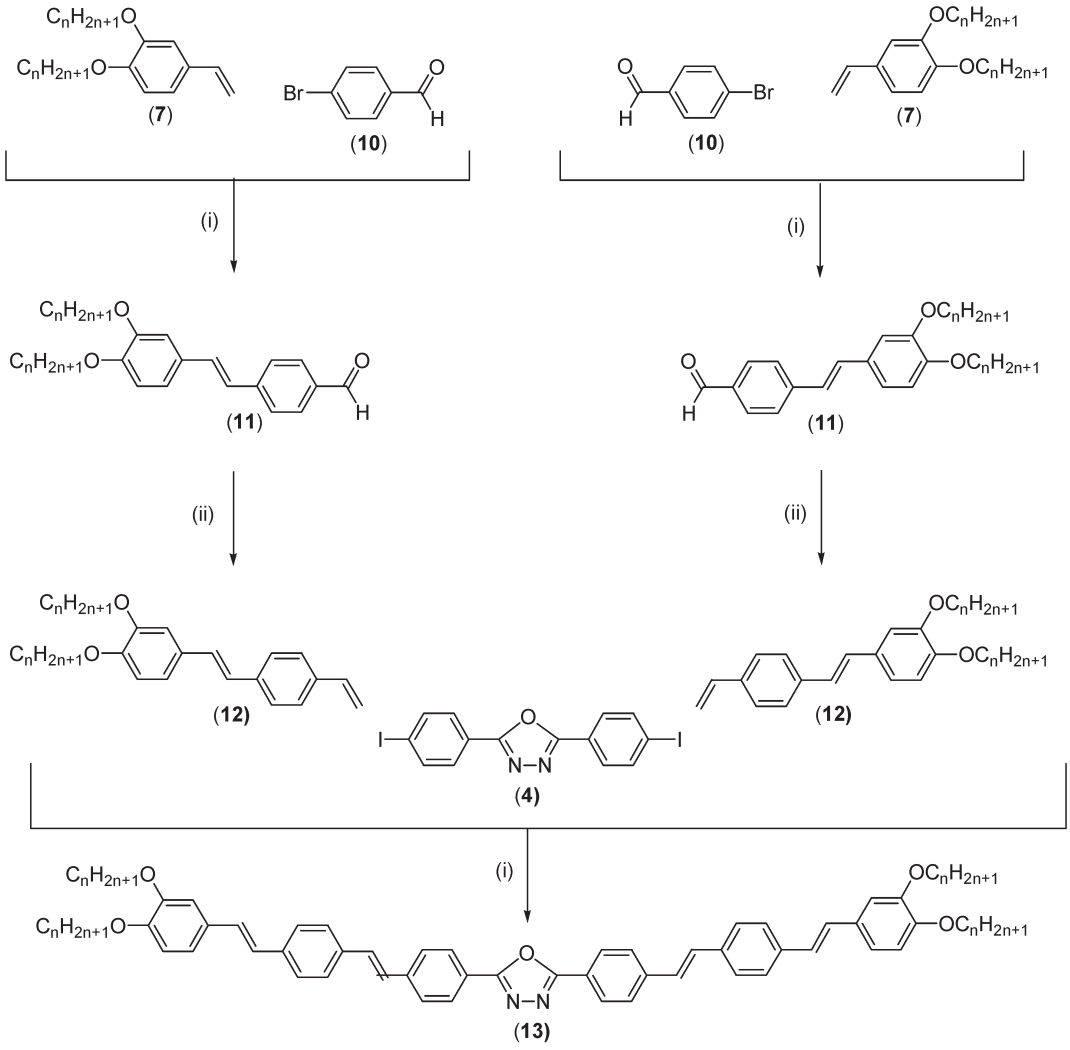

Scheme 2. Reagents and conditions: (i) Hermann's catalyst, DMF, $N(C_2H_5)_3$; (ii) $CH_3P(C_6H_5)_3Br$, $KOC(CH_3)_3$, DME.

Williamson ether synthesis [41] with THP-protected 8-bromooctanol (**15**) prepared in the usual way [43] from 8-bromooctan-1-ol (**14**) to yield the THP-protected benzaldehyde (**16**), which was converted in a Wittig reaction [40] into the THP-protected styrene (**17**). A Heck reaction [39, 42] between the THP-protected styrene (**17**) and bis(4-iodophenyl)-1,3,4-thiadiazole (**4**; X=S) yielded the tetra-alcohol (**18**), which was esterified in the usual way [44] using methacrylic acid, DCC and DMAP to yield the desired thiadiazole (**19**) with a methacrylate group at the end of each of the four terminal chains. Deprotection of the hydroxy-groups was achieved during the Heck reaction work-up with acid.

The 2,5-substituted [1, 3, 4]-thiadiazole (**20**) was prepared in one step in a Suzuki aryl–aryl cross-coupling reaction [45, 46] between bis(4-iodophenyl)-1,3,4-thiadiazole (**4**; X=S) and 3,4-dialkoxyphenylboronic acid available from another programme [19].

2.2.1. 4-Iodobenzoyl chloride (2). Oxalyl chloride (25.2 g, 0.2 mol) was added dropwise to a mixture of 4-iodobenzoic acid (**1**; 25.0 g, 0.1 mol) and DMF (few drops) in dichloromethane (200 cm^3) at room temperature (RT). The reaction mixture was stirred overnight under anhydrous conditions and evaporated down under reduced pressure to give the chloride as a brown solid, which was used without further purification. Yield 25.0 g (94%).

2.2.2. 1,2-Di(4-iodobenzoyl)hydrazine (3). A solution of 4-iodobenzoyl chloride (**2**; 25.0 g, 0.09 mol) in THF (250 cm^3) was added dropwise to a solution of hydrazine in THF (100 cm^3, 1M solution) at RT. After 24 h the solid precipitate was filtered off, washed with water (2×150 cm^3) and dried in vacuo. The raw product was purified by recrystallization from ethyl acetate. Yield 17.4 g (73%), m.p. >275°C. ^{1}H NMR

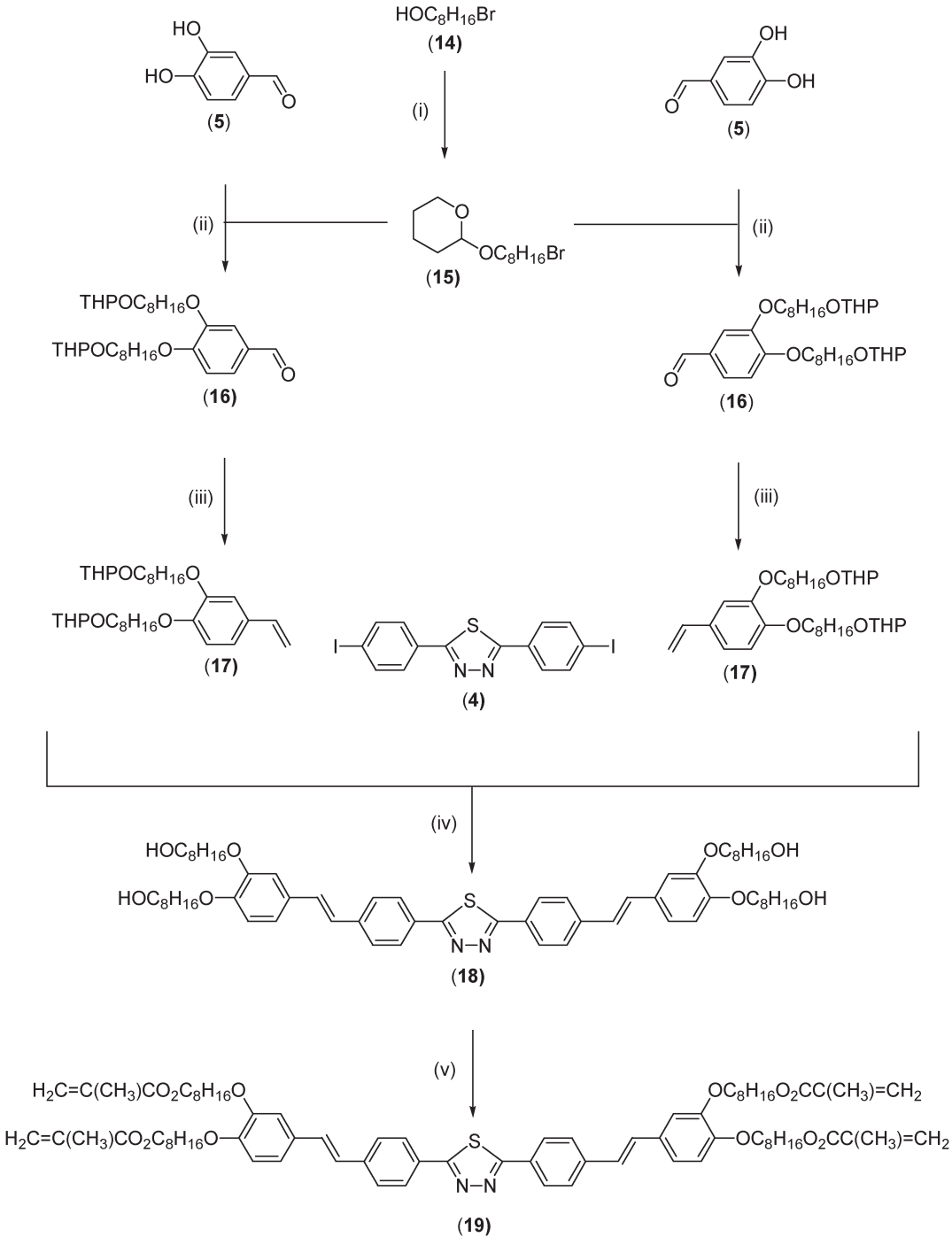

Scheme 3. Reagents and conditions: (i) PTSA, DHP, CH_2Cl_2; (ii) K_2CO_3, $C_2H_5COCH_3$; (iii) $CH_3P(C_6H_5)_3Br$, $KOC(CH_3)_3$, DME; (iv) Hermann's catalyst, DMF, $N(C_2H_5)_3$; (v) $H_2C{=}C(CH_3)CO_2H$, DCC, DMAP, DMF.

($CDCl_3$) δ_H: 10.6 (2H, s), 7.8 (8H, dd). IR ν_{max} (cm^{-1}): 3204 (s), 1605 (s), 1554 (s), 1495 (m), 1461 (s), 1263 (m), 1116 (w), 1055 (w), 1005 (m), 837 (m), 737 (m), 703 (w), 649 (m), 547 (w), 454 (w). MS (m/z): 492 (M^+, M100), 247, 231, 203, 127, 76.

2.2.3. 2,5-Bis(4-iodophenyl)-1,3,4-oxadiazole (4; X=O). Phosphoryl chloride (100 cm^3) was added to 1,2-di(4-iodobenzoyl)hydrazine (**3**; 7.0 g, 14 mmol), and the mixture heated under reflux for 28 h. The reaction mixture was poured slowly into cold water (800 cm^3),

the brown precipitate filtered off and the raw product purified by recrystallisation from DMF to yield a pale brown crystalline solid. Yield 5.0 g (75%), m.p. >275°C. Purity 100% (GC). ^{1}H NMR (DMSO) δ_H: 8.05 (4H, d), 7.90 (4H, d). IR ν_{max} (cm^{-1}): 1598 (m), 1537 (w), 1475 (s), 1408 (m), 1274 (m), 1074 (m), 1004 (s), 963 (m), 832 (s), 732 (s), 489 (s), 422 (w). MS (m/z): 474 (M^+, M100), 231, 203, 127, 76.

2.2.4. 2,5-Bis(4-iodophenyl)-1,3,4-thiadiazole (4; X=S). Phosphorus pentasulfide (1.0 g, 4.5×10^{-3} mol) was added carefully to a stirred suspension of 1,2-bis(4-iodobenzoyl)hydrazine (**3**; 1.5 g, 3.0 mmol) in pyridine (10 cm^3). The resultant reaction mixture was heated at 100°C for 16 h. The cooled mixture was added to ice (200 g), the resultant precipitate filtered off, washed with water (50 cm^3) and purified by recrystallization from DMF. Yield 0.7 g (50%), m.p. >275°C. Purity 100% (GC). ^{1}H NMR (DMSO) δ_H: 7.9 (4H, d), 7.7 (4H, d). IR ν_{max} (cm^{-1}): 3395 (w), 1585 (m), 1482 (w), 1425 (s), 1387 (s), 1249 (m), 1088 (m), 1057 (m), 1007 (m), 985 (s), 820 (s), 782 (m), 596 (s), 496 (m), 464 (m). MS (m/z): 490 (M^+, M100), 363, 261, 247, 229, 203, 176, 150, 134.

2.2.5. 3,4-Dioctyloxybenzaldehyde (6; $R_1=R_2=C_8H_{17}O$; R_3=H). A mixture of 1-bromooctane (11.19 g, 57.9 mmol), 3,4-dihydroxybenzaldehyde (**5**; $R_1=R_2=C_8H_{17}O$; R_3=H; 2.00 g, 14.5 mmol), potassium carbonate (7.99 g, 57.9 mmol) and butanone (200 cm^3) was heated under reflux for 24 h. The inorganic material was filtered off from the cooled reaction mixture and the filtrate poured onto water and then extracted with ethyl acetate (3×100 cm^3). The combined organic extracts were washed by sodium hydroxide solution (10%, 100 cm^3) and with water (150 cm^3) and then dried ($MgSO_4$). The raw product was purified by column chromatography on silica gel using a 1:1 mixture of dichloromethane and hexane as eluent and recrystallisation from ethanol. Yield: 4.37 g, 83.4%. ^{1}H NMR (270.05 MHz, $CDCl_3$, TMS) δ_H: 9.85 (1H, s, HCO), 7.4 (2H, m, Ar–H), 6.95 (1H, d, J=6.75 Hz, Ar–H), 4.06 (4H, qua, J=5.4 Hz, $ArOCH_2$), 1.85 (4H, sex, J=5.4 Hz, $ArOCH_2CH_2$), 1.5–1.3 (10H, m, CH_2), 0.99 (6H, m, CH_3). IR (KBr) ν_{max} (cm^{-1}): 2960 (C–H, stretching, CH_3, s), 2880 (CH_2, C–H, sym, str), 1700 (C=O, stretching, s), 1600 (C=C, skeletal, vibrations, s), 1520 (C=C, skeletal, in-plane, var), 1480, 1440, 1400 (C–O, stretching, sym, s), 1280, 1240 (C–O, str, Ar–O), 1180, 1140 (alkyl–O, sym, str), 1060, 1020 (Ar–O, sym, str.), 820 (C–H, out-of-plane, bend). MS (m/z): 362 (M^+), 249, 138 (100 %), 109, 71, 57.

2.2.6. 3,4-Dioctyloxystyrene (7; $R_1=R_2=C_8H_{17}O$; R_3=H). A mixture of 1,2-dimethoxyethane (150 cm^3), 3,4-dioctyloxybenzaldehyde (**6**; $R_1=R_2=C_8H_{17}O$; R_3=H; 4.37 g, 12.1 mmol) and methyltriphenylphosphonium bromide (8.62 g, 24 mmol) were then introduced into the flask. After stirring for 15 min, potassium *tert*-butoxide (4.06 g, 36 mmol) was added in portions over 15 min. The resultant reaction mixture was stirred for 4 h at RT and then water (50 cm^3) and dilute hydrochloric acid (20 cm^3) were added to the reaction mixture, which was extracted with diethyl ether (3×100 cm^3). The combined ether layers were washed with brine (3×50 cm^3) and dried ($MgSO_4$). The raw product was purified by column chromatography using a 1:1 mixture of dichloromethane and hexane as eluent to yield a colourless liquid. Yield: 1.94 g, 44.7%. ^{1}H NMR (399.65 MHz, $CDCl_3$, TMS) δ_H: 6.98–6.81 (3H, m, Ar–H), 6.68–6.58 (1H, m, CH=C), 5.58 (1H, d, J=8.1 Hz, CH=C), 5.12 (1H, d, J=5.4 Hz, C=CH_2) 4.0 (4H, m, $ArOCH_2$), 1.81 (4H, m, $ArOCH_2CH_2$), 1.50–1.25 (20H, m, CH_2), 0.89 (6H, m, CH_3). IR (film) ν_{max} (cm^{-1}): 2940 (C–H, stretching, CH_2, asym, s), 2880 (C–H, stretching, CH_3, sym, s), 1610, 1580 (C=C, skeletal, vibrations, s), 1520 (C=C, skeletal, in-plane, var), 1480, 1440 (C–H, deformation, CH_3, CH_2, asym, m), 1400 (C–O, stretching, w), 1270, 1240 (C–O, stretching aryl-O, s), 1140, 1040, 1000 (C–O, stretching, alkyl-O), 900, 800 (C–H, out-of-plane, deformation). MS (m/z): 360 (M^+), 304, 248, 192, 162, 136 (100 %), 119, 91.

2.2.7. 2,5-Bis{4-[(*E*)-(3,4-dioctyloxyphenyl)ethenyl]phenyl}-1,3,4-oxadiazole (8; $R_1=R_2=C_8H_{17}O$; R_3=H). A mixture of 3,4-dioctyloxystyrene (**7**; $R_1=R_2=C_8H_{17}O$; R_3=H; 0.40 g, 1.1 mmol), 2,5-bis(4-iodophenyl)-1,3,4-oxadiazole (**4**; X=O; 0.25 g, 0.53 mmol), palladium(II) acetate (4.0 mg, 1.78×10^{-5} mol), tris(*o*-tolyl)phosphine (0.030 g, 9.9×10^{-5} mol) and triethylamine (0.50 g, 5.0 mmol) in DMF (10 cm^3) was heated at 80°C for 24 h. DCM was added to the cooled reaction mixture until most of the solid had dissolved and any remaining palladium was filtered off. The filtrate was added dropwise to concentrated hydrochloric acid (36%, 150 cm^3) and water (200 cm^3) with stirring and the resultant precipitate filtered off, washed with water (50 cm^3) and dried in vacuo. The raw product was purified by column chromatography [silica gel, DCM:petroleum ether (fraction 40–60°C) 1:5] and by recrystallization from ethanol to yield the desired final product. Yield 0.07 g (14%). ^{1}H NMR (CD_2Cl_2) δ_H: 8.1 (4H, d), 7.65 (4H, d), 7.15 (2H, d, J=16 Hz), 7.10 (6H, m), 6.87 (2H, d, J=16 Hz), 4.0 (8H, m), 1.8 (8H, 2xt offset), 1.5 (8H, 2xt offset), 1.3 (32H, m), 0.88 (12H, t). IR ν_{max} (cm^{-1}): 3431 (w), 2928 (s), 2857 (s), 1597 (m),

1517 (s), 1469 (m), 1433 (m), 1393 (w), 1315 (w), 1271 (s), 1175 (m), 1141 (s), 1065 (m), 1016 (m), 960 (m), 843 (m), 800 (w), 599 (w). Combustion analysis: calculated, C 79.27%, H 9.23%, N 2.98%; found, C 78.26%, H 9.35%, N 2.98%.

2.2.8. 2,5-Bis{4-[(*E*)-(3,4-dioctyloxyphenyl)ethenyl] phenyl}-1,3,4-thiadiazole (9; $R_1=R_2=C_8H_{17}O$; $R_3=H$). A mixture of 3,4-dioctyloxystyrene (**7**; $R_1=R_2=C_8H_{17}O$; $R_3=H$; 0.75 g, 2.1 mmol), 2,5-bis(4-iodophenyl)-1,3,4-thiadiazole (**4**; X=S; 0.35 g, 7.1×10^{-4} mol), palladium(II) acetate (4.0 mg, 1.78×10^{-5} mol), tris(*o*-tolyl)phosphine (0.030 g, 9.9×10^{-5} mol) and triethylamine (2 cm^3) in DMF (10 cm^3) was heated at 100°C for 4 days. The reaction mixture was allowed to cool before filtering and washing through with hot chloroform (200 cm^3). The filtrate was added to dilute hydrochloric acid (18%, 200 cm^3) and the organic layer separated off, washed with dilute hydrochloric acid (18%, 2×150 cm^3) and water (2×150 cm^3) then dried ($MgSO_4$). The solution was concentrated onto silica gel and purified by column chromatography [silica gel, 20% ethyl acetate in petroleum ether (fraction 40–60°C) gradients to chloroform] and by recrystallization from a 1:1 mixture of ethanol:chloroform to yield the desired final product. Yield 0.32 g (47%). ^{1}H NMR ($CDCl_3$) δ_H: 7.99, (4H, d), 7.60 (4H, d), 7.15 (2H, d, J=16 Hz), 7.11 (2H, d), 7.07 (2H, dd), 6.98 (d, 2H, J=16 Hz), 6.87 (2H, d), 4.05 (8H, 2xt offset), 1.85 (8H, m), 1.48 (8H, m), 1.31 (32H, m), 0.89 (12H, t). IR ν_{max} (cm^{-1}): 3443 (m), 2929 (s), 2857 (s), 1595 (m), 1569 (m), 1518 (s), 1435 (m), 1253 (s), 1142 (s), 1066 (w), 960 (w), 841 (w). Combustion analysis: calculated, C 77.94%, H 9.07%, N 2.93%; found, C 77.48%, H 9.07%, N 2.85%.

2.2.9. 4-[(*E*)-2-(3,4-Dioctoxyphenyl)ethenyl]benzaldehyde (11; n=8). A mixture of 3,4-dioctyloxystyrene (**7**; $R_1=R_2=C_8H_{17}O$; $R_3=H$; 2.36 g, 6.55 mmol), 4-bromobenzaldehyde (**10**; 1.46 g, 7.86 mmol), Herrman's catalyst (0.09 g, 9.8×10^{-5} mol) and triethylamine (1.66 g, 16.4 mmol) in DMF (50 cm^3) was heated at 100°C for 4 days. The reaction mixture was allowed to cool before filtering and washing through with hot chloroform (200 cm^3). The filtrate was added to dilute hydrochloric acid (18%, 50 cm^3) and the organic layer separated off, washed with dilute HCl (18%, 2×150 cm^3) and water (2×50 cm^3) then dried ($MgSO_4$). The product was purified by the column chromatography on silica gel using a mixture (1:4) of dichloromethane and hexane as the eluent and by recrystallization from ethanol to give a yellow solid. Yield: 2.28 g, 75%. ^{1}H NMR (399.65 MHz, $CDCl_3$, TMS) δ_H: 9.98 (1H, s, OCH), 7.85 (2H, d, J=8.3 Hz, Ar–H), 7.62 (2H, d, J=8.3 Hz, Ar–H), 7.22–6.50 (5H, m, CH=CH, Ar–H), 4.04 (4H, m, $ArOCH_2$), 1.85 (4H, m, CH_2), 1.54–1.29 (20H, m, CH_2), 0.89 (6H, m, CH_3). IR (KBr) ν_{max} (cm^{-1}): 2940 (C–H, stretching, CH_3, s), 2860 (C–H, stretching, CH_2, sym, s), 1700 (C=O, stretching, s), 1600 (C=C, skeletal, vibrations, s), 1520 (C=C, skeletal, in-plane, var), 1480, 1440, 1400 (C–O, stretching, sym, s), 1280, 1240 (C–O, stretching, aryl-O, s), 1180, 1140 (C–H, skeletal, s), 1060, 1020 (C–O, stretching, alkyl-O), 980 (C–H, in-plane, deformation), 840 (C–H, out-of-plane, deformation). MS (m/z): 464 (M^+), 408, 351, 296, 251, 240 (100 %), 219, 181, 165, 138, 126, 91, 71.

2.2.10. 3,4-Dioctyloxystyryl-4-styrene (12, n=8). 1,2-Dimethoxyethane (50 cm^3) was placed in a round bottomed flask and stirred vigorously for 30 min to remove oxygen. 4-[(*E*)-2-(3,4-Dioctoxyphenyl)ethenyl] benzaldehyde (**11**, n=8; 0.75 g, 1.62 mmol) and methyltriphenylphosphonium bromide (1.15 g, 3.23 mmol) were then introduced into the flask and the resultant mixture stirred for 15 min. Potassium *tert*-butoxide (0.54 g, 4.85 mmol) was then added in portions over 15 min and the resultant mixture stirred for 4 h at RT. Water (50 cm^3) and dilute hydrochloric acid (10 cm^3) were added to the reaction mixture, which was extracted with diethyl ether (3×50 cm^3). The combined ether layers were washed with brine (3×50 cm^3) and then dried ($MgSO_4$). The raw product was purified by the column chromatography using a 1:1 mixture of dichloromethane and hexane as eluent and recrystallization from ethanol to give the desired product. Yield: 0.42 g, 56.76%. ^{1}H NMR (399.65 MHz, $CDCl_3$, TMS) δ_H: 7.42 (4H, m, Ar–H, C=C), 7.04 (3H, m, Ar–H, C=C), 6.89 (2H, m, Ar–H), 6.71 (1H, m, $CH=CH_2$), 5.75 (1H, d, J=17.5 Hz, $C=CH_2$), 5.24 (1H, d, J=11.47 Hz, $C=CH_2$), 4.03 (4H, m, $ArOCH_2$), 1.84 (4H, m, CH_2), 1.52–1.29 (20H, m, CH_2), 0.89 (6H, t, J=6.07 Hz, CH_3). IR (KBr) ν_{max} (cm^{-1}): 2940 (C–H, stretching, CH_2, asym, s), 2880 (C–H, stretching, CH_3, sym, s), 1600 (C=C, skeletal, vibrations, s), 1520 (C=C, skeletal, in-plane, var), 1470, 1430 (C–H, bend, asym, m, CH_3), 1400 (C–O, stretching, w), 1290, 1260, 1240 (C–O, stretching aryl-O, s), 1140 (C–O, stretching, s, sym), 1060, 1030, (C–O, stretching, alkyl-O), 970, 920 (C–H, in-plane, deformation), 860, 800 (C–H, out-of-plane, deformation). MS (m/z): 462 (M^+), 406, 350, 322, 294, 249, 238 (100 %), 209, 191, 177, 165, 152, 141, 115, 97, 83, 69.

2.2.11. 2,5-Bis{4-[(*E*)-2-(3,4-dioctyloxystyryl)styryl]phenyl} -[1, 3, 4]-oxadiazole (13, n=8). A mixture of

3,4-dioctyloxystyryl-4-styrene (**12**; $n=8$; 0.42 g, 9.09×10^{-4} mol), 2,5-bis(4-iodophenyl)-1,3,4-oxadiazole (**4**; X=O; 0.22 g, 4.54×10^{-4} mol), Herrman's catalyst (0.006 g, 6.8×10^{-6} mol), and triethylamine (0.11 g, 1.14 mmol) in DMF (50 cm^3) was heated at 100°C for 4 days. The reaction mixture was allowed to cool before filtering and washing through with hot chloroform (200 cm^3). The filtrate was added to dilute HCl (18%, 50 cm^3) and the organic layer separated off, washed with dilute hydrochloric acid (18%, 2×50 cm^3) and water (2×50 cm^3) then dried ($MgSO_4$). The raw product was purified by the column chromatography on silica gel using a 1:1 mixture of dichloromethane and hexane as the eluent and by recrystallization from a mixture 1:2 of dichloromethane and methanol to yield the desired final product. Yield: 0.1 g, 19.6%. ^{1}H NMR (399.65 MHz, $CDCl_3$, TMS) δ_H: 8.12 (2H, m, Ar–H), 7.88 (1H, m, C=C), 7.66 (2H, m, Ar–H), 7.52 (4H, m, Ar–H, C=C), 7.23–6.86 (6H, m, CH=CH, Ar–H), 4.04 (4H, m, $ArOCH_2$), 1.83 (4H, m, CH_2), 1.52–1.26 (20H, m, CH_2), 0.89 (6H, m, CH_3). IR (KBr)ν_{max} (cm^{-1}): 2940 (C–H, stretching, CH_3, s), 2880 (C–H, stretching, CH_2, sym, s), 1600 (C=N, stretching, v), 1520 (C=C, skeletal, in-plane, var), 1480, 1430 (C–H, bend, CH_3, asym, m), 1400 (C–O, stretching, w), 1270, 1230 (C–O, stretching, aryl-O, s), 1140, 1080, 1010 (C–O, stretching, alkyl-O), 960 (C–H, in-plane, deformation), 840 (C–H, out-of-plane, deformation). MS (APCI) m/z: 1143 (M^++H), 810 (100 %), 683, 627, 553, 475, 421. CHN expected % (found %): C 81.96 (69.84); H 8.58 (7.25); N 2.45 (3.26).

2.2.12. 2-(8-Bromooctyloxy)tetrahydropyran (15). A solution of 2,3-dihydropyran (2.3 g, 0.027 mol), 8-bromooctan-1-ol (**14**; 5.0 g, 0.024 mol) and PTSA (0.25 g) in DCM (50 cm^3) was stirred for 20 h. The solvent was removed in vacuo and the product purified by dry flash chromatography (silica gel, hexane:DCM 1:1) to yield a colourless oil. Yield 6.3 g (90%). ^{1}H NMR ($CDCl_3$) δ_H: 4.57 (1H, t), 3.87 (1H, m), 3.73 (1H, m), 3.49 (1H, m), 3.38 (3H, m), 1.85 (3H, m), 1.71 (1H, m), 1.55 (6H, m), 1.38 (8H, m). IR ν_{max} (cm^{-1}): 2933 (s), 2859 (s), 1463 (m), 1351 (m), 1261 (m), 1204 (m), 1124 (s), 1075 (s), 1031 (s), 988 (m), 906 (m), 869 (w), 645 (w). MS (m/z): 293 (M^+), 191, 101, 85 (M100), 69, 55.

2.2.13. 3,4-Bis[8-(tetrahydropyran-2-yloxy)octyloxy] benzaldehyde (16). A mixture of 2-(8-bromooctyloxy)tetrahydropyran (**15**; 6.3 g, 21 mmol), 3,4-dihydroxybenzaldehyde (**5**; 1.2 g, 8.4 mmol), and potassium carbonate (3.7 g, 27 mmol) in butanone was heated under reflux for 20 h. Excess potassium carbonate was filtered off and the solution concentrated onto silica gel for purification by column chromatography (silica gel, hexane:DCM 3:1 gradients to DCM:ethyl acetate 3:1) to yield a colourless liquid. Yield 4.5 g (94%). ^{1}H NMR ($CDCl_3$) δ_H: 7.41 (1H, dd), 7.39 (1H, d), 6.94 (1H, d), 4.57 (2H, t), 4.06 (4H, $2\times$t offset), 3.87 (2H, m), 3.73 (2H, m), 3.49 (2H, m), 3.39 (2H, m), 1.60 (36H, m). IR ν_{max} (cm^{-1}): 2936 (s), 1693 (s), 1593 (s), 1512 (s), 1438 (s), 1350 (m), 1269 (s), 1204 (m), 1136 (s), 1077 (s), 1032 (s), 906 (w). MS (m/z): 562 (M^+), 479, 393, 364, 249, 138, 85 (M100).

2.2.14. 3,4-Bis[8-(tetrahydropyran-2-yloxy)octyloxy] styrene (17). Potassium *tert*-butoxide (1.3 g, 11.2 mmol), was added slowly to a stirred mixture of 3,4-bis[8-(tetrahydropyran-2-yloxy)octyloxy]benzaldehyde (**16**; 4.9 g, 8.0 mmol) and methyltriphenylphosphonium bromide (3.4 g, 9.6 mmol) in DME (100 cm^3). After 2 h additional methyltriphenylphosphonium bromide (0.5 g), and potassium *tert*-butoxide (0.5 g) were added. After stirring for a further 1 h, DCM (150 cm^3) was added and the solution washed with dilute HCl (10%, 100 cm^3) followed by water (100 cm^3) and the organic layer dried ($MgSO_4$) and concentrated onto silica gel for purification by column chromatography (silica gel, hexane:ethyl acetate 4:1) to yield a colourless oil. Yield 3.7 g (82%). ^{1}H NMR ($CDCl_3$) δ_H: 6.96 (1H, d), 6.91 (1H, dd), 6.81 (1H, d), 6.63 (1H, quart), 5.58 (1H, d), 5.12 (1H, d), 4.57 (2H, t), 4.00 (4H, $2\times$t offset), 3.87 (2H, m), 3.72 (2H, m), 3.49 (2H, m), 3.39 (6H, m), 1.62 (32H, m). IR ν_{max} (cm^{-1}): 2940 (s), 2862 (s), 1604 (w), 1514 (m), 1470 (m), 1352 (w), 1264 (s), 1204 (m), 1138 (s), 1078 (s), 1032 (s), 989 (m), 813 (w). MS (m/z): 560 (M^+), 477, 393, 264, 136 (M100).

2.2.15. 2,5-Bis(4-{(*E*)-[3,4-di-(8-hydroxyoctyloxy)phenyl] ethenyl}phenyl)-1,3,4-thiadiazole (18). A mixture of 3,4-bis[8-(tetrahydropyran-2-yloxy)octyloxy]styrene (**17**; 1.61 g, 3.0 mmol), 2,5-bis(4-iodophenyl)-1,3,4-thiadiazole (**4**; X=S; 0.50 g, 1.0 mmol), Herrmann's catalyst (0.015 g, 1.1×10^{-5} mol) and triethylamine (0.5 g) in DMF (40 cm^3) was heated at 80°C for 48 h. More 3,4-bis[8-(tetrahydropyran-2-yloxy)octyloxy]styrene (**17**; 0.16 g, 0.4 mmol) and Herrmann's catalyst (0.01 g, 1.1×10^{-5} mol) were added to the cooled reaction mixture and the mixture heated at 90°C for a further 24 h. Herrmann's catalyst (0.01 g, 1.1×10^{-5} mol) was added to the cooled reaction mixture, which was then heated at 110°C for a further 24 h. Water (100 cm^3) and dilute hydrochloric acid (20%, 50 cm^3) were added and the product was extracted into a 4:1 chloroform–methanol mixture (3×50 cm^3). The product was concentrated onto silica gel for purification by column chromatography (silica gel, hexane:DCM 3:1 gradient to warm chloroform:methanol 4:1). Yield 0.5 g (48 %), m.p.

200°C. ^{1}H NMR (DMSO) δ_H: 8.04 (4H, d), 7.79 (4H, d), 7.41 (4H, s overlapping d, J=16 Hz), 7.29 (2H, d, J=16 Hz), 7.17 (2H, d), 7.00 (2H, d), 4.07 (4H, t), 4.01 (4H, t), 3.39 (8H, quart), 1.75 (8H, m), 1.41 (40H, m). IR ν_{max} (cm^{-1}): 3352 (m), 2932 (s), 2857 (s), 1631 (m), 1517 (s), 1470 (m), 1435 (m), 1252 (s), 1138 (s), 1057 (s), 962 (m), 843 (m).

2.2.16. 2,5-Bis(4-{(*E*)-[3,4-di-(8-methacryloyloxyoctyloxy) phenyl]ethenyl}phenyl)-1,3,4-thiadiazole (19). A mixture of 2,5-bis(4-{(*E*)-[3,4-di-(8-hydroxyoctyloxy)phenyl] ethenyl}phenyl)-1,3,4-thiadiazole (**18**; 0.28 g, 2.7×10^{-4} mol), DCC (0.28 g, 1.4 mmol), methacrylic acid (0.2 g, 2.3 mmol) and DMAP (0.02 g, 1.6×10^{-4} mol) in DMF was stirred for 48 h. Additional DCC (2 g), methacrylic acid (2 g) and DMAP (0.5 g) were added and the resultant mixture heated at 40°C for 48 h and then at 50°C for a further 48 h. The solvent was removed in vacuo, DCM (10 cm^3) was added and any insoluble material filtered off. The solution was concentrated onto silica gel and purified by column chromatography (silica gel, hexane:DCM 2:1 gradients to pure DCM) followed by recrystallization from ethanol. The product was dissolved in DCM (5 cm^3) and passed through a microfilter (Whatman, 0.45 μm, PTFE) and the solution concentrated to a green solid which was further purified by recrystallization from ethanol. Yield 120 mg (34%). ^{1}H NMR (CD_2Cl_2) δ_H: 7.99 (4H, d), 7.63 (4H, d), 7.19 (2H, d, J=16 Hz), 7.13 (2H, d), 7.08 (2H, dd), 7.03 (2H, d, J=16 Hz), 6.88 (2H, d), 6.06 (4H, m), 5.54 (4H, m), 4.11 (8H, 2 × t offset), 4.04 (4H, t), 4.01 (4H, t), 1.92 (12H, t), 1.84 (8H, m), 1.68 (8H, m), 1.50 (8H, m), 1.38 (24H, m). IR ν_{max} (cm^{-1}): 3429 (m, broad), 2927 (s), 2857 (s), 2372 (m), 1719 (s), 1595 (m), 1521 (m), 1462 (m), 1434 (m), 1406 (w), 1324 (m), 1253 (m), 1170 (s), 1058 (m), 815 (w). APCI-MS (m/z): 1292 (M$^+$, M100), 1206, 1120. Combustion analysis: calculated, C 72.53%, H 7.96%, S, 2.48%; found, C 72.92%, H 8.32%, S 2.50%.

2.2.17. 2,5-Bis(3′,4′-dioctyloxybiphenyl-4-yl)-1,3,4-thiadiazole (20). A mixture of 2,5-bis(4-iodophenyl)-1,3,4-thiadiazole (**4**; X=S; 0.50 g, 1.0 mmol), (3,4-dioctyloxyphenyl)-boronic acid (0.95 g, 3.0 mmol), tribasic potassium phosphate (1.9 g, 9.0 mmol), and tetrakis(triphenylphosphine)palladium(0) (0.18 g, 1.5×10^{-4} mol) in DME (60 cm^3) was heated under reflux for 24 h. The solvent was removed in vacuo and DCM (100 cm^3) added. The solution was washed with brine (2×150 cm^3), water (2×150 cm^3), dried ($MgSO_4$) and then concentrated onto silica gel for purification by column chromatography (silica gel, DCM) and recrystallisation from ethanol:chloroform to yield a the desired final product. Yield 0.08 g (9%). ^{1}H NMR ($CDCl_3$) δ_H: 8.06 (4H, d), 7.68 (4H, d), 7.19 (4H, m), 6.97 (2H d), 4.07 (8H, 2 × t offset), 1.85 (8h, 2 × t offset), 1.50 (8H, 2 × t offset), 1.30 (32H, m), 0.89 (12H, t). IR ν_{max} (cm^{-1}): 2928 (s), 2856 (s), 1598 (m), 1530 (m), 1508 (s), 1469 (m), 1442 (m), 1329 (m), 1257 (s), 1205 (s), 1147 (s), 1065 (m), 832 (m), 799 (m), 721 (w). APCI-MS (m/z): 904 (M$^+$). Combustion analysis: calculated, C 77.12%, H 9.15%, N 3.10%, S 3.55%; found, C 76.84%, H 9.15%, N 2.93%, S 3.44%.

2.3. *Mesomorphic properties*

A nematic (N) phase was observed for some of the compounds prepared, e.g. the oxadiazole **13** (n=6). A Schlieren texture with 2-brush and 4-brush disclinations are observed for the N phase observed between crossed polarizers (see figure 1). Small droplets are seen on cooling slowly from the isotropic phase on forming the N phase. Several compounds exhibit a smectic A (SmA) and a smectic C (SmC) phase, e.g. the dicatenar oxadiazole (**8**; R_1=R_2=H; R_3=$C_nH_{2n+1}O$; n=14) and the much longer tetracatenar oxadiazoles (**13**; n=2, 4, 6, 8).

Other homologues of this series just exhibit an enantiotropic SmA phase, which exhibits the focal conic texture as well as optically extinct areas in the same sample (see figure 2). The simultaneous presence of these two types of texture is characteristic of the calamitic SmA phase. Elliptical and hyperbolic lines of optical discontinuity characteristic of focal conic defects are also observed. The focal conics develop dark bars across their backs on cooling into the SmC phase and isotropic areas develop a Schlieren texture with only four point brushes at this transition (see figure 3) due to the optical biaxial nature of the SmC phase.

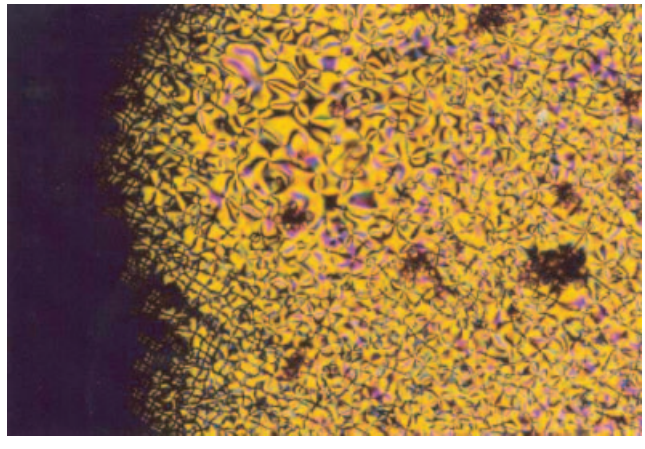

Figure 1. Schlieren texture of the nematic phase of compound **13** (n=6) formed on cooling from the isotropic liquid, on a glass substrate (× 160).

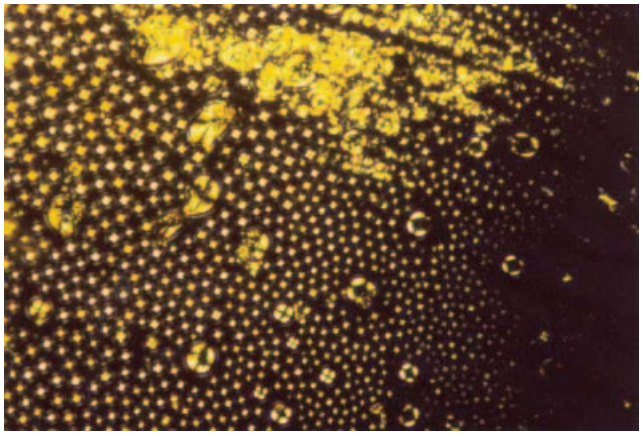

Figure 2. The focal-conic fan and homeotropic textures of the smectic A phase of compound **13** (n=6) at 185°C formed on cooling from the nematic phase, on a glass substrate (× 160).

A Schlieren texture could also be observed directly on cooling from the isotropic (I) liquid for several of the polycatenars prepared, e.g. the tetracatenar oxadiazoles (**8**; $R_1=R_2=C_nH_{2n+1}O$; $R_3=H$; $n=6$ and 8) (see figure 4). No droplets are seen on cooling slowly from the I phase on forming the SmC phase and only disclinations with four-point brushes were observed for the resultant Schlieren texture with no isotropic areas.

The textures of the columnar phases (Col) exhibited by the final compounds are varied (see figures 5–8). Typical textures include the mosaic texture and the fan-like texture exhibited by the tetracatenar oxadiazoles (**8**; $R_1=R_2=C_{12}H_{25}O$; $R_3=H$) with very long chains (see figure 5) and the thiadiazole (**9**; $R_1=R_2=C_8H_{17}O$; $R_3=H$) with shorter chains, (see figures 6–8). These

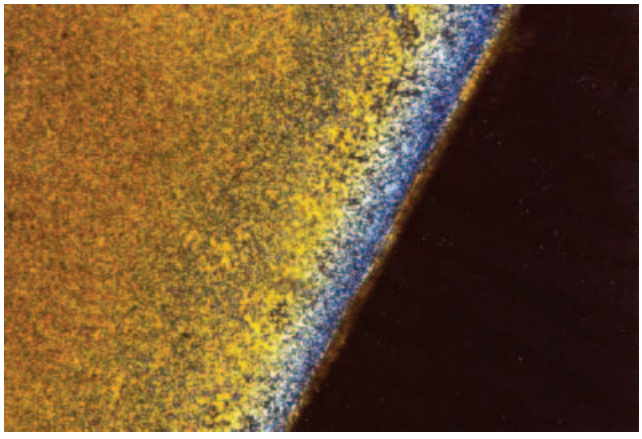

Figure 3. The Schlieren texture of the smectic C phase of the tetracatenar oxadiazole (**13**, n=6) at 140°C formed on cooling from the smectic A phase, on a glass substrate (× 160).

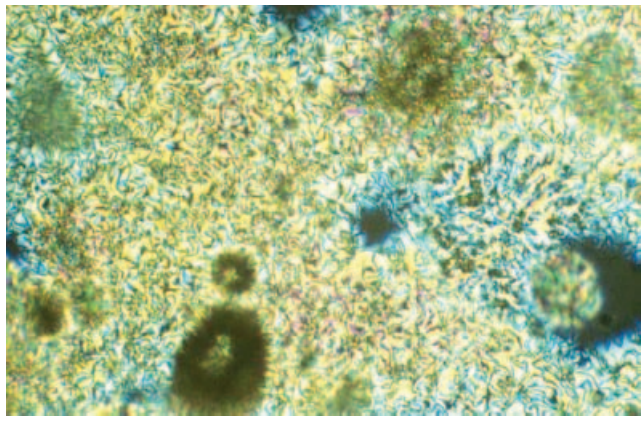

Figure 4. Schlieren texture of the smectic C phase of the tetracatenar oxadiazole (**8**; $R_1=R_2=C_8H_{17}O$; $R_3=H$) on a glass substrate (× 160).

textures are characteristic of the ordered and disordered hexagonal columnar phases. However, it is difficult to characterize the exact type of columnar mesophase exhibited by these compounds with absolute certitude without recourse to X-ray studies. Therefore, the transitions in the tables are reported as columnar phases and no distinction is made between ordered and disordered columnar phases. The texture shown in figure 8 is probably that of a SmC phase (see section 3). The transitions observed using optical microscopy were confirmed using differential scanning calorimetry (DSC). Where the liquid crystal transition temperatures could not be obtained directly by optical microscopy then the values from DSC analysis corresponding to the onset peak are used. The enthalpy values for the phase transitions of the final compounds are also recorded in tables 1–8.

Figure 5. Fan texture of the hexagonal columnar phase exhibited by the tetracatenar oxadiazole (**8**; $R_1=R_2=C_{12}H_{25}O$; $R_3=H$).

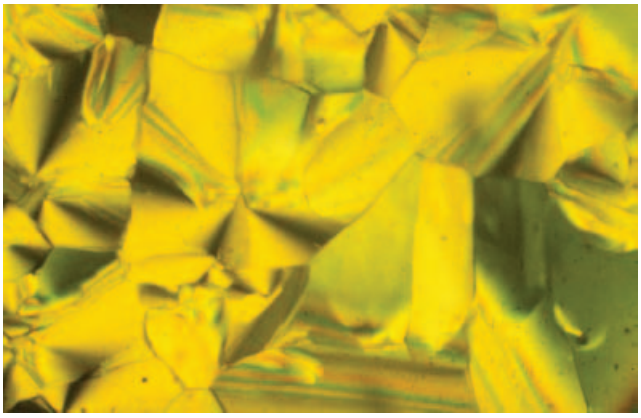

Figure 6. Fan texture of the hexagonal columnar phase exhibited by the tetracatenar thiadiazole (**9**; $R_1=R_2=C_8H_{17}O$; $R_3=H$).

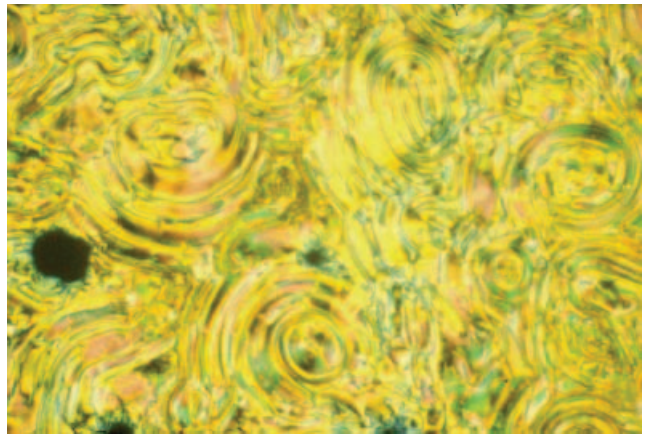

Figure 8. Texture of the third liquid crystal phase exhibited by tetracatenar thiadiazole (**9**; $R_1=R_2=C_8H_{17}O$; $R_3=H$) after cooling from the columnar phase.

3. Results and discussion

The phase transition temperatures and enthalpies of the dicatenar 2,5-bis{4-[(*E*)-2-(4-alkoxyphenyl)vinyl] phenyl}-[1, 3, 4]-oxadiazoles (**8**; $R_1=R_3=H$; $R_2=C_nH_{2n+1}O$; $n=2$, 4, 6, 8, 10, 12, 14) are collated in table 1. These dicatenars are clearly classical rod-like mesogens with a linear rod-like aromatic core and two alkoxy chains in terminal positions. Therefore this series of liquid crystals only exhibits lamellar mesophases, i.e. the SmA and SmC phases. The melting and clearing points generally decrease as the series is ascended from short to longer chains. The reduction in the melting point is due to dilution of the aromatic cores by an increasing concentration of flexible aliphatic chains with low melting points.

Table 2 reports the transition temperatures and enthalpies of a homologous series of the tetracatenar 2,5-bis{4-[(*E*)-2-(3,4-dialkoxyphenyl)vinyl]phenyl}-[1, 3, 4]-oxadiazoles (**8**; $R_1=R_2=C_nH_{2n+1}O$; $R_3=H$; $n=2$, 4, 6, 8, 10, 12, 14, 16). The melting point decreases by over 100°C as the chain length increases from very high values for the homologues with short chains ($n=2$ and 4). These homologues ($n=2$ and 4) are solids and do not exhibit observable mesomorphic behaviour due to a limited amount of supercooling below the melting point. Homologues with longer chains ($n=6$ and 8) show a lamellar SmC phase at elevated temperatures. Homologues even with longer chains ($n=10$, 12, 14 and 16) only exhibit an enantiotropic columnar phase over a relatively large temperature range. The clearing point of the columnar phase increases marginally with increasing chain length. The melting and clearing endotherms are all first order transitions and possess typical values for the type of mesophase observed, e.g. the enthalpy of the melting points is much larger than that of the clearing

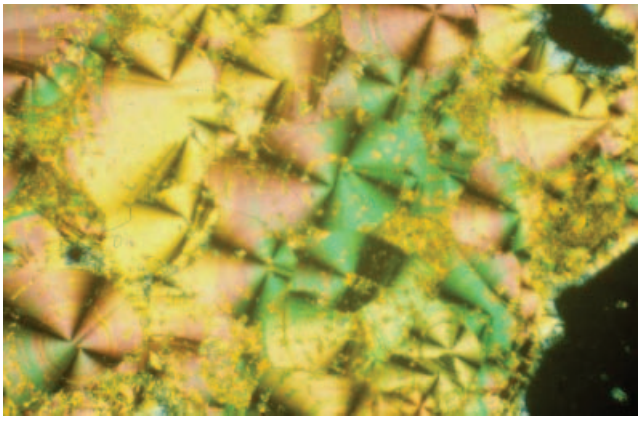

Figure 7. Circular domain texture exhibited by the tetracatenar oxadiazole (**9**; $R_1=R_2=C_8H_{17}O$; $R_3=H$).

Table 1. Transition temperatures (°C) and some enthalpies of transition (kJ mol^{-1}, in square brackets) for 2,5-bis{4-[(*E*)-2-(4-alkoxyphenyl)vinyl]phenyl}-[1, 3, 4]-oxadiazole (**8**; $R_1=R_3=H$; $R_2=C_nH_{2n+1}O$).

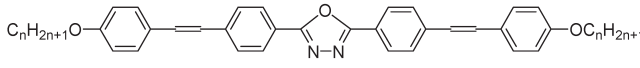

n	Cr		SmC		SmA		I
2	.	154 [17.03]		–		–	.
4	.	163 [35.85]		–	.	215 [2.95]	.
6	.	148 [24.99]		–	.	210	.
8	.	152 [37.75]		–	.	204	.
10	.	148 [35.42]		–	.	200 [2.38]	.
12	.	135 [22.26]		–	.	197 [2.44]	.
14	.	125 [26.60]	.	(180)	.	195 [4.69]	.

( ) represents a monotropic transition temperature (°C).

Table 2. Transition temperatures (°C) and some enthalpies of transition (kJ mol^{-1}, in square brackets) for 2,5-bis{4-[(*E*)-2-(3,4-dialkoxyphenyl)vinyl]phenyl}-[1, 3, 4]-oxadiazole (**8**; $R_1=R_2=C_nH_{2n+1}O$; $R_3=H$) [18].

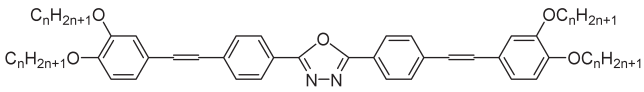

n	Cr		Col		SmC		I
2	.	186 [21.93]		–		–	.
4	.	150 [35.01]		–		–	.
6	.	120 [34.31]		–	.	122 [4.36]	.
8	.	108 [54.87]		–	.	120 [3.07]	.
10	.	86 [43.58]	.	112 [2.23]		–	.
12	.	90 [70.53]	.	128 [2.91]		–	.
14	.	98 [78.10]	.	130 [2.12]		–	.
16	.	98 [134.58]	.	139 [4.44]		–	.

Table 3. Transition temperatures (°C) and some enthalpies of transition (kJ mol^{-1}, in square brackets) for the 2,5-bis{4-[(*E*)-2-(3,4,5-trisalkoxyphenyl)vinyl]phenyl}-[1, 3, 4]-oxadiazole (**8**; $R_1=R_3=R_3=C_nH_{2n+1}O$) [18].

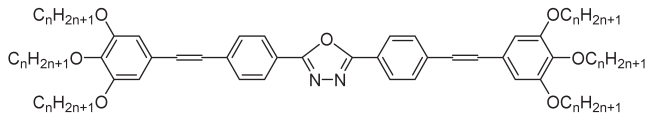

n	Cr		Col		I
2	.	125 [21.02]		–	.
4	.	165 [30.43]		–	.
6	.	118 [22.05]		–	.
8	.	88 [18.50]	(.	77) [2.65]	.
9	.	77 [30.45]	.	78 [4.28]	.
10	.	70 [7.05]	.	80 [1.92]	.
11	.	65 [54.74]	.	80 [5.19]	.
12	.	78 [18.65]	.	83 [3.50]	.
14	.	81 [81.16]	.	83 [3.91]	.

( ) represents a monotropic transition temperature (°C).

points (see table 2). These molecules can be regarded as amphiphilic in nature [13]. Segregation of the aromatic and aliphatic parts of the molecule occurs in the mesophase to produce a curvature at the aromatic-aliphatic interface. As the chain length is increased so the curvature is increased, resulting in the columnar mesophases being stabilised at the expense of the lamellar mesophases [15]. The average number of molecules in a disk making up a column of catenar compounds was found to be four for biforked mesogens such as these with four terminal alkoxy chains [13]. The paraffinic volume is large enough for long chains to allow the four-molecule clusters, which pack in a two dimensional arrays, to form columns [13, 14]. Long alkyl chains with high flexibility are more likely to favour the association of molecules in discs making up the columnar mesophase [16]. The interactions between the aromatic cores are very weak due to the presence of a large concentration of bulky paraffinic chains. This columnar structure is clearly different from those formed by conventional discoid molecules, such as triphenylenes and coronenes [15].

The transition temperatures and enthalpies of the hexacatenar 2,5-bis{4-[(*E*)-2-(3,4,5-*tris*-alkoxyphenyl)-vinyl]phenyl}-[1, 3, 4]-oxadiazoles (**8**; $R_1=R_2=R_3=C_nH_{2n+1}O$; n=2, 4, 6, 8, 9, 10, 11, 12, 14) are collected in table 3. The homologues with relatively short alkoxy chains (n=2, 4, 6) are solids with a high melting point. A limited amount of supercooling below the melting point prevents the observation of monotropic mesophases. The melting points generally decreases with increasing chain length with a minimum in the middle of the series (n=11). With the exception of the octyl homologue (n=8), which shows a monotropic columnar phase on cooling below the melting point, the other homologues with longer chains (n=9, 10, 11, 12 and 14) exhibit an enantiotropic columnar phase and the melting point of these compounds is lower than 90°C. No lamellar phases, such as the SmA or SmC phases, are observed for this series of hexacatenars. The low clearing points of this homologous series is clearly attributable to the large number (six) of the paraffinic chains and the lateral *meta* positions for four of them [13]. The melting points are all first-order transitions and the transition from the mesophase to the isotropic liquid is also weakly first order. The clearing point enthalpies are relatively small in comparison with the melting enthalpies as expected. The melting points and the clearing points of the *tetracatenar* molecules listed in table 2 are much higher than those of the *hexacatenar* molecules collated in table 3. The temperature range of the columnar phase for the former is generally larger than that of the latter. The homologues (**8**; $R_1=R_2=R_3=C_nH_{2n+1}O$; n=8, 9, 10, 11, 12, 14) of the hexacatenar series exhibit only columnar phases due to the presence of six chains [13]. Most of the tetracatenars (**8**; $R_1=R_2=C_nH_{2n+1}O$; $R_3=H$; n=10, 12, 14, 16) shown in table 2 also exhibit a columnar phase, although two homologues (**8**; $R_1=R_2=C_nH_{2n+1}O$; $R_3=H$; n=6 and 8) with shorter chains exhibit a SmC phase. This is clearly due to the lower number of chains and shorter chain lengths for these homologues and the differences in curvature [13].

The mesomorphic behaviour of four tetracatenar compounds is compared in table 4, which lists the transition temperatures for two oxadiazoles (**8**;

Table 4. Transition temperatures (°C) and enthalpies of transition ($J\,g^{-1}$, in square brackets) for oxadiazoles (**8**; X=O; $R_1=R_2=C_nH_{2n+1}O$; $R_3=H$) and the thiadiazoles (**9**; X=S; $R_1=R_2=C_nH_{2n+1}O$; $R_3=H$).

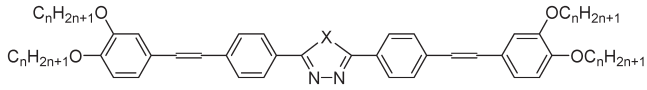

n	X	Cr		SmC_3		Col_2		Col_1		I
8	O	.	108 [54.87]	.	120 [3.07]		–		–	.
8	S	.	152 [58.6]	.	177 [0.17]	.	194 [4.7]	.	201 [2.70]	.
12	O	.	78 [18.65]		–		–	.	83 [3.50]	.
12	S	.	137 [47.0]		–	.	148 [2.8]	.	213 [3.00]	.

$R_1=R_2=C_{12}H_{25}O$; $R_3=H$; $n=8$ and 12) and the corresponding thiadiazioles (**9**; $R_1=R_2=C_{12}H_{25}O$; $R_3=H$; $n=8$ and 12) where the only difference is the presence of a sulfur atom in place of the oxygen atom in the heterocyclic ring in the centre of the molecule. The mesomorphism observed and the values of the transition temperatures are consistent with the concept of increasing curvature between aliphatic and aromatic moieties with increases in the chain length and temperature. The increase in chain length, and hence curvature favours the formation of columnar phases to the detriment of lamellar smectic phases, e.g. the C_8 oxadiazole (**8**; $R_1=R_2=C_8H_{17}O$; $R_3=H$) exhibits only a SmC phase (see figure 4), whereas the C_{12} oxadiazole (**8**; $R_1=R_2=C_{12}H_{25}O$; $R_3=H$) with much longer alkoxy chains only exhibits a columnar phase (see figure 5). However, the situation may be more complex as is often the case for catenar compounds [13]. For example, the C_8 thiadiazole (**9**; $R_1=R_2=C_8H_{17}O$; $R_3=H$) exhibits two columnar phases *and* probably also a SmC phase, characteristic of low curvature, below the columnar phases on cooling (see figures 6–8). Although it is difficult to identify the SmC phase with certainty, a Schlieren texture with four-point brush, is observed on shearing the original paramorphophic texture shown in figure 8. However, this unusual phase behaviour of the C_8 thiadiazole (**9**; $R_1=R_2=C_8H_{17}O$; $R_3=H$) is analogous to other 2mp–2mp tetracatenar compounds reported in the literature [13]. The enthalpy of transition from the SmC phase into the columnar phase for **9** ($R_1=R_2=C_8H_{17}O$; $R_3=H$) is very low. This is characteristic of lamellar–columnar transitions and is thought to be due to non-drastic structural changes [13]. The paraffinic volume becomes large enough at the transition temperature to allow the four-molecule clusters resulting from an enhanced undulation to twist slightly and form a paraffinic sheath, which leads to the formation of a supramolecular columnar structure. A comparison of the C_{12} oxadiazole (**8**; $R_1=R_2=C_{12}H_{25}O$; $R_3=H$) and the C_{12} thiadiazole (**9**; $R_1=R_2=C_{12}H_{25}O$; $R_3=H$) reveals only a hexagonal columnar phase for the oxadiazole, whereas the thiadiazole compound exhibits both a hexagonal columnar phase and the tilted columnar phase characteristic of lower curvature.

The oxadiazoles (**8**; $R_1=R_2=C_nH_{2n+1}O$; $R_3=H$; $n=8$ and 12) shown in table 4 exhibit much lower transition temperatures than those of the corresponding thiadiazoles (**9**; $R_1=R_2=C_nH_{2n+1}O$; $R_3=H$; $n=8$ and 12). This is probably due to the more bent i.e. non-linear molecular structure of the oxadiazoles (see figure 9), which results in lower molecular packing efficiency. It should be noted that mesomorphic behaviour and phase transition temperatures depend not only on the number and length of the aliphatic of chains, but also on the number of aromatic rings in the molecular core as well as the shape of the core.

The transition temperatures and enthalpies of the hexacatenar 2,5-bis{4-[(*E*)-2-(3,4,5-trisalkoxyphenyl) vinyl]phenyl}-[1, 3, 4]-thiadiazoles (**9**; $R_1=R_2=R_3=C_nH_{2n+1}O$; $n=2$, 4, 6, 8, 11) are listed in table 5. The

Table 5. Transition temperatures (°C) and some enthalpies of transition ($kJ\,mol^{-1}$, in square brackets) for 2,5-bis{4-[(*E*)-2-(3,4,5-trisalkoxyphenyl)vinyl]phenyl}-[1, 3, 4]-thiadiazole (**9**; $R_1=R_2=R_3=C_nH_{2n+1}O$).

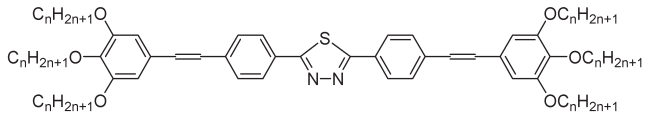

n	Cr		Col		I
2	.	210 [13.14]		–	.
4	.	130 [14.85]		–	.
6	.	60 [8.01]	.	80 [1.17]	.
8	.	65	.	85 [1.77]	.
11	.	75 [82.95]	.	90 [1.86]	.

Table 6. Transition temperatures (°C) and some enthalpies of transition (kJ mol^{-1}, in square brackets) for 2,5-bis{4-[(*E*)-2-(3,4-dialkoxystyrene)styryl]phenyl}-[1, 3, 4]-oxadiazole (**13**).

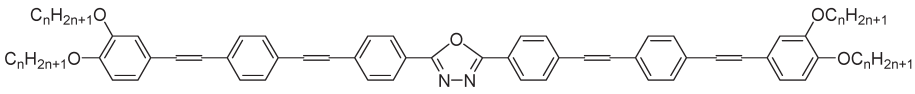

n	Cr		SmC		SmA		N		I
2	.	255 [26.47]		–	.	275 [1.5]		–	.
4	.	185 [7.66]		–	.	230 [5.1]		–	.
6	.	118 [21.95]	.	145 [8.5]	.	215 [0.4]	.	225 [0.42]	.
8	.	157 [27.53]	.	170	.	180		–	.
10	.	125 [26.44]	.	175 [8.3]		–		–	.
14	.	100 [32.85]	.	120		–		–	.

thiadiazoles (**9**; $R_1=R_2=R_3=C_nH_{2n+1}O$; n=2, 4, 6, 8, 11) exhibit a similar mesomorphic behaviour to that of the corresponding oxadiazoles (**8**; $R_1=R_2=R_3=C_nH_{2n+1}O$; n=2, 4, 6, 8, 9, 10, 11, 12, 14) shown in table 3, although fewer homologues are reported for the thiadiazole series. The melting points decrease with increasing chain length as usual. Homologues with long alkoxy chains (n=6, 8, 11) exhibit an enantiotropic columnar phase, the clearing point of which increases somewhat with increasing chain length. The clearing point temperatures are similar to those of the oxadiazole series (**8**; $R_1=R_2=R_3=C_nH_{2n+1}O$; n=2, 4, 6, 8, 9, 10, 11, 12, 14), whereas the melting points of most of the homologues of the hexacatenar thiadiazoles (**9**; $R_1=R_2=R_3=C_nH_{2n+1}O$; n=2, 4, 6, 8) are generally lower than those of the corresponding hexacatenar oxadiazoles. Therefore, the range of the columnar phase of the thiadiazoles is somewhat larger than that of the corresponding oxadiazoles.

The difference in shape of the aromatic core of the hexacatenar oxadiazoles and the corresponding thiadiazoles (see figure 9) does not appear to influence the mesomorphism or the transition temperatures of these two series. This appears to depend much more on the ratio of the aliphatic and aromatic components of the molecules and the number and position of the alkoxy chains. This interpretation is consistent with the fact that only columnar mesophases are observed for the hexacatenar thiadiazoles (**9**; $R_1=R_2=R_3=C_nH_{2n+1}O$; n=6, 8, 11) and oxadiazoles (**8**; $R_1=R_2=R_3=C_nH_{2n+1}O$; n=8, 9, 10, 11, 12, 14) with relatively long alkoxy chains. No other type of mesophase is observed, e.g. lamellar SmA or SmC phases. This is also consistent with the normal behaviour of many other hexacatenar compounds reported in the literature [13, 14]. Usually, it is considered that the hexacatenar molecules associate into clusters in the columnar phase, with the column section being formed by three molecules on average [14]. The differences in shape of the aromatic core of the thiadiazoles and the oxadiazoles may well be compensated for in such a supramolecular arrangement. In addition, due to the bulky paraffinic chains, the interactions between cores are very weak perpendicular to the *xz*-plane; i.e. along the column axis parallel to the disk-like layers [13]. Therefore, the columnar mesophase observed in both series is not highly ordered and the hexagonal columnar phase is generally observed. The main area per paraffinic chain increases with chain length, corresponding to an increase of the curvature between the aromatic and the paraffinic moieties and so

Table 7. Transition temperatures (°C) for tetracatenar (**9**; $R_1=R_2=C_8H_{17}O$; R_3=H), tetrahydroxy intermediate (**18**) and the reactive mesogen (**19**).

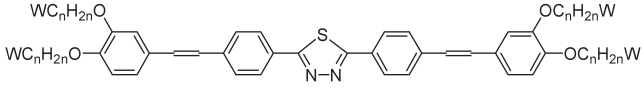

	W	Cr		SmC		Col_2		Col_1		I
9	H	.	152	.	177	.	194	.	201	.
18	OH	.	200		–		–		–	.
19	$H_2C=C(CH_3)CO_2$-	.	106		–		–	.	133	.

Table 8. Transition temperatures (°C) for the tetracatenar phenylenevinylene thiadiazole (**9**; $R_1=R_2=C_8H_{17}O$; $R_3=H$) and the bisbiphenyl thiadiazole (**20**).

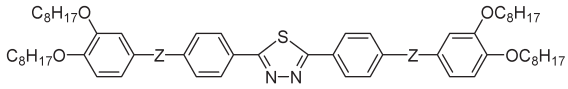

	Z	Cr		SmC		Col_2		Col_1		I
9	–CH=CH–	.	152	.	177	.	194	.	201	.
20	–	.	133	.	160		–		–	.

Figure 9. Comparison of the structures of thiadiazole (left) and oxadiazole compounds as modelled using Chem3D Pro software. The internal C–S–C bond angle is ~148° for the thiadiazole and the internal C–O–C bond angle is ~127° for the oxadiazole.

columnar mesophases are formed directly from the isotropic liquid for heacatenars with long chains [13].

The transition temperatures and enthalpies of the oxadiazoles (**13**; $n=2$, 4, 6, 8, 10, 12, 14) with seven aromatic rings and four more rigid CH=CH bridges in the aromatic core are listed in table 6. The compounds (**13**) exhibit the highest shape anisotropy, i.e. length-to-breadth ratio, of all the polycatenar series studied and as a consequence exhibit a range of lamellar phases including the SmA and SmC phase as well as the N phase. No columnar mesophases are observed. The melting and clearing points generally decrease from very high values for homologues with short alkoxy chains with increasing chain length as usual. The SmA phase is replaced by the SmC phase for homologues with the longest alkoxy chains. Space filling requirements probably lead to the formation of the tilted SmC phase rather than the orthogonal SmA phase. Thermal degradation makes exact determination of the clearing point of some of these materials problematical and a nematic phase may well be exhibited by more than the one homologue ($n=6$) shown in table 6, but cannot be observed due to decomposition at lower temperatures. The shape anisotropy and the rigidity of the rod-like part of the molecule play an important role in the formation of lamellar smectic mesophases. The SmA phase observed for homologues with shorter chains ($n=2$, 4, 6, 8) is gradually replaced by the SmC phase for

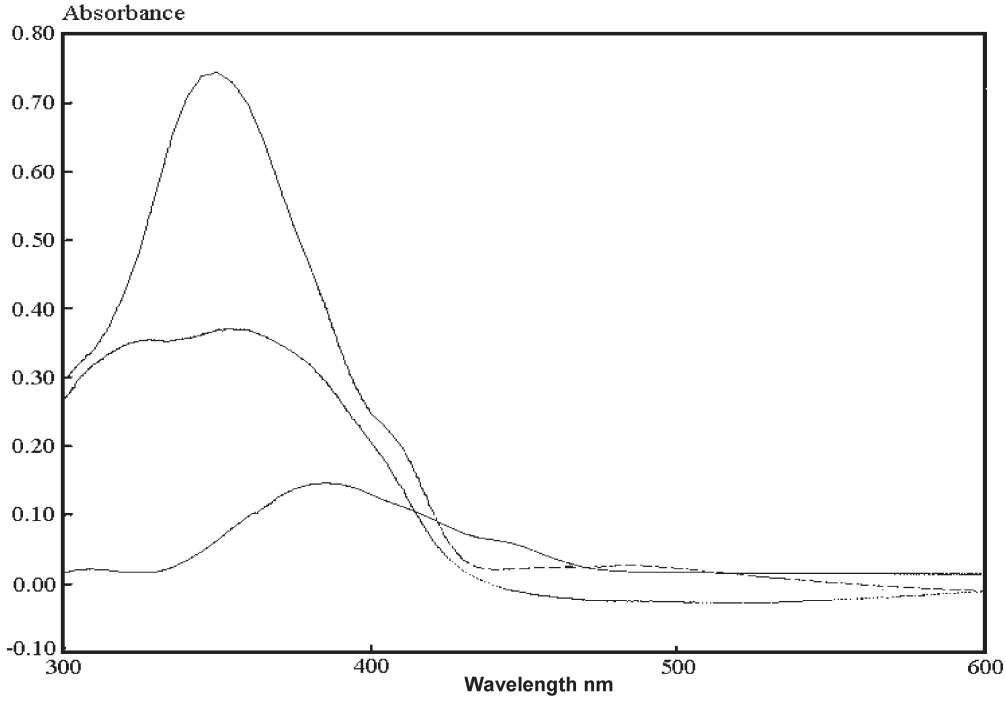

Figure 10. Absorption spectra of the tetracatenar oxadiazoles [**8**; $R_1=R_2=C_nH_{2n+1}O$; $R_3=H$; $n=8$ (peak at 0.75) and $n=12$ (peak at 0.34)] and the analogous tetracatenar thiadiazole [**9**; $R_1=R_2=C_nH_{2n+1}O$; $R_3=H$; $n=8$ (peak at 0.14)].

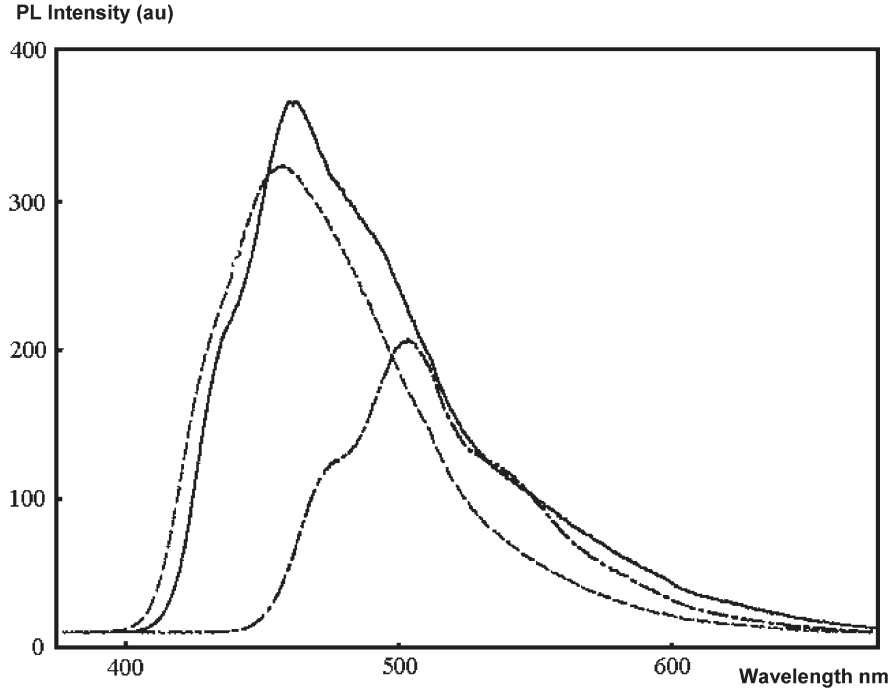

Figure 11. PL spectra for the tetracatenar oxadiazoles [**8**; $R_1=R_2=C_nH_{2n+1}O$; $R_3=H$; $n=8$ (dashed line) and $n=12$ (solid line)] and the analogous tetracatenar thiadiazole [**9**; $R_1=R_2=C_nH_{2n+1}O$; $R_3=H$; $n=8$ (dash-dot line)].

homologues with longer chains. The high degree of flexibility of long alkoxy chains as well as dilution effects on the interaction between the aromatic cores by the aliphatic chains may well contribute to the lower clearing points observed for homologues with long chains. The enthalpy of fusion of the oxadiazoles (**13**; n=2, 4, 6, 8, 10, 12, 14) is larger than that of the clearing points, as expected.

The phase transition temperatures for the reactive mesogen (**19**) with a polymerizable methacrylate group ($W=H_2C=C(CH_3)CO_2$) at the end of each of the four octyloxy chain are shown in table 7. As expected, the tetracatenar compound (**19**) exhibits a hexagonal columnar liquid crystalline phase as does the corresponding tetracatenar (**9**; $R_1=R_2=C_8H_{17}O$; $R_3=H$) with four terminal octyloxy chains in the same positions, i.e., the only difference is a hydrogen atom (W=H) in place of the methacrylate group. The transition temperatures of the reactive mesogen (**19**) are relatively low when compared to those of the corresponding tetracatenar (**9**; $R_1=R_2=C_8H_{17}O$;

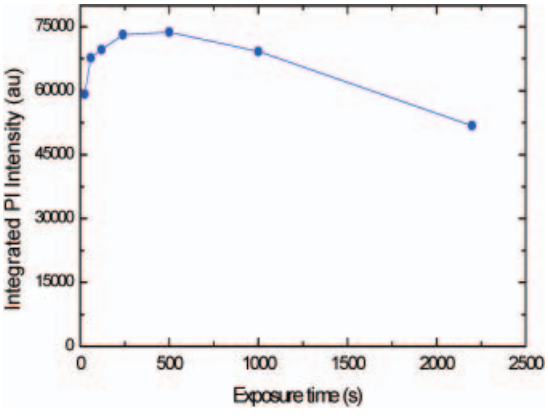

Figure 12. Change in the PL spectrum of the reactive mesogen **19** during the photochemical polymerization process.

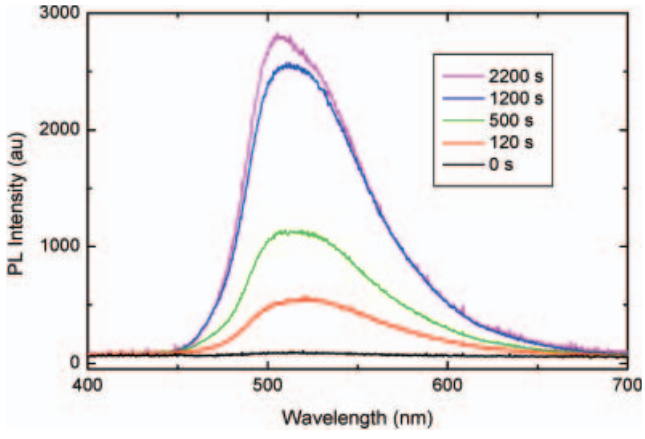

Figure 13. PL spectra from the reactive mesogen **19** exposed with UV light of wavelength 300 nm and intensity 50 mW cm^{-2} for 120 s, 500 s, 1200 s and 2200 s after dissolution in chloroform.

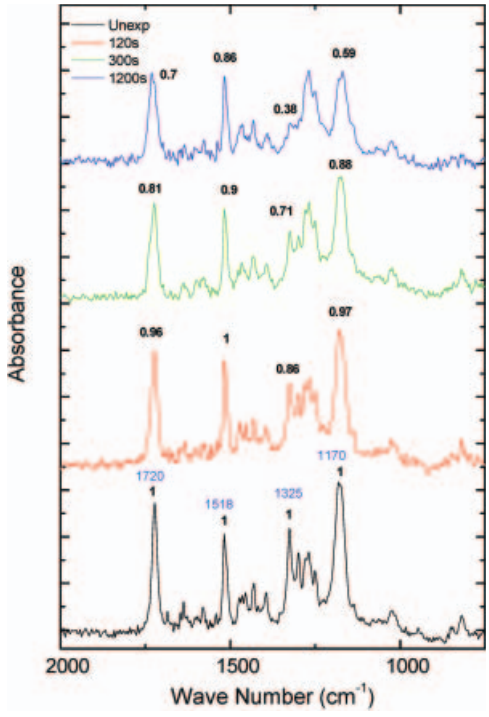

Figure 14. FTIR spectra of films of the reactive mesogen **19** unexposed and exposed with UV light at 300 nm for 120 s, 300 s and 1200 s. The numbers in black show the relative intensities of the labelled transitions following irradiation.

R_3=H) with four terminal octyloxy chains in the same positions. This is most probably due to the bulky methacrylate groups causing a reduced packing efficiency due to significant steric effects and the space filling requirements of the methacrylate groups. The tetrahydroxy intermediate (**18**) is non-mesomorphic with a high melting point due to hydrogen bonding between the terminal hydroxy groups (W=OH).

The thiadiazole (**20**) with no ethylenic linkages only exhibits a SmC phase (table 8), unlike the analogous thiadiazole (**9**; R_1=R_2=$C_8H_{17}O$; R_3=H) incorporating two additional unsaturated carbon–carbon double bonds. This compound also probably exhibits a SmC phase as well as two columnar phases (see table 4). The absence of columnar phases for the thiadiazole (**20**) with no ethylenic linkages is probably due to the shorter core length. It is known that liquid crystalline phase formation is strongly dependent on the length of the molecular core in polycatenar systems [13], although it is not clear why the shorter core should favour the formation of the smectic C phase in this example.

3.1. *Physical properties*

The absorption spectra of the oxadiazoles (**8**; R_1=R_2=$C_nH_{2n+1}O$; R_3=H; n=8 and 12) and the thiadiazole (**9**; R_1=R_2=$C_8H_{16}O$; R_3=H) are shown in figure 10. The absorption spectra show a peak absorbance wavelength of around 350 nm for the oxadiazoles (**8**; R_1=R_2=$C_nH_{2n+1}O$; R_3=H; n=8 and 12). This increases to approximately 380 nm for the thiadiazole (**9**; R_1=R_2=$C_8H_{17}O$; R_3=H). This increase is probably due to a lowering of the π–π^* band gap energy caused by electron donation into the aromatic system by the sulphur atom. The photoluminescence PL spectra for the compounds are shown in figure 11. Compounds **8** (R_1=R_2=$C_nH_{2n+1}O$; R_3=H; n=8 and 12) show a similar emission peak in the PL spectrum at ~460 nm. The thiadiazole (**9**; R_1=R_2=$C_8H_{17}O$; R_3=H) shows a red-shifted peak at ~500 nm.

In order to assess the photopolymerization process, a 50 nm thick film of the reactive mesogen (**19**) containing 1 wt % of a commercially available photoinitiator (Irgacure) was prepared. The film was divided into eight zones, which were exposed to a 300 nm UV laser of intensity 50 mW cm^{-2} for various lengths of time. Interestingly, as figure 12 shows, the PL intensity increased over the first few minutes of exposure. This may be due to the photopolymerization process eliminating some of the PL quenching sites in the polycrystalline film. Later, the PL intensity decreased with increasing exposure implying some degradation. This result is consistent with previous work which showed some photodegradation of a fluorene reactive mesogen with methacrylate photoreactive groups following UV irradiation [47]. No degradation was found when dienes were used as the photoreactive groups. In order to assess qualitatively the degree of polymerisation, the sample was dissolved in chloroform for 10 s following exposure in order to remove low-molecular-weight organic material and then dried in a flow of dry nitrogen. The absorbance maximum of the film irradiated for 1000 s was reduced by 25% by washing suggesting that most of the material had been rendered insoluble by the polymerization process. The absorbance spectrum for samples exposed for 1000 s and 2200 s were very similar, indicating a saturation of the polymerisation process. This is limited in polymer networks generally due to the enormous viscosity of highly cross-linked networks and the probability of finding an adjacent reactive monomer. Figure 13 shows PL spectra from the irradiated zones after washing. A low PL intensity implies removal of the chromophore by washing. These results suggest that a reasonably high degree of polymerisation had occurred after an exposure time of around 1000 s.

Figure 14 shows FTIR spectra from a thin film of the reactive mesogen (**19**) for different photopolymerization times. During exposure, a shift in the peak at 1720 cm^{-1}

to 1730 cm^{-1} occurs. This peak corresponds to the methacrylate carbonyl stretch and a shift would be expected during polymerization due to the transition from α,β-conjugated ester to non-conjugated ester. The peaks at 1325 cm^{-1} and 1170 cm^{-1} both decrease significantly during exposure. Both of these transitions are identified with the methacrylate group, the former is due to a $=CH_2$ deformation and the latter to a C-O stretch [48]. The reduction in oscillator strength is consistent with the loss of the α,β-unsaturated ester by polymerization. A smaller photoinduced decrease in the transition at 1518 cm^{-1}, which originates from the aromatic rings of the chromophore, is found; this confirms a small degradation of the aromatic core of the molecule.

4. Conclusions

The dicatenar oxadiazoles prepared exhibit lamellar phases, the tetracatenar oxadiazoles with two or more alkoxy chains exhibit both lamellar and columnar phases, i.e. intermediate behaviour, whereas the hexacatenar oxadiazoles with six alkoxy chains possess only columnar phases. The corresponding tetracatenar and hexacatenar thiadiazoles only form columnar phases. The more linear molecular structure of the core of polycatenar thiadiazoles leads to higher clearing points for the tetracatenars, but makes little difference for the hexacatenars where the influence of the number and length of the alkoxy chains dominates the liquid crystalline behaviour. Increasing the shape anisotropy of the tetracatenar oxadiazoles by the presence of two additional phenylenevinylene groups to create a more calamitic, rod-like molecular shape leads to the formation of lamellar phases. The phase transition temperatures decrease as expected with increasing number of chains from dicatenars to tetracatenars to hexacatenars. A photopolymerizable analogue of these new classes of organic materials has been photochemically polymerized to form a crosslinked liquid crystalline polymer network without significant photochemical degradation.

Acknowledgments

We express our thanks to the EPSRC for funding. The University of Hull is also thanked for postgraduate studentships (GJR and CW). We would also like to thank B. Worthington (^{1}H NMR) and K. Welham (MS) for spectroscopic measurements.

References

[1] M. O'Neill, S.M. Kelly. *Adv. Mater.*, **15**, 1135 (2003).
[2] D. Adam, D. Haarer, F. Closs, T. Frey, D. Funhoff, K. Siemensmeier, P. Schumacher, H. Ringsdorf. *Ber. Buns. Phys. Chem.*, (1993); **97**, 1366 *Phys. Rev. Lett.*, **70**, 457 (1993).
[3] C. Catry, M. van der Auweraer, F.C. de Schryver, H. Bengs, K. Häussling, O. Karthaus, H. Ringsdorf. *Makromol. Chem.*, **194**, 2985 (1993).
[4] D. Adam, P. Schumacher, J. Simmerer, K. Häussling, K. Siemensmeier, K.H. Etzbach, H. Ringsdorf, D. Haarer. *Nature.*, **371**, 141 (1994).
[5] E.O. Arikainen, N. Boden, R.J. Bushby, J. Clemments, B. Movaghar, W. Wood. . J. *Mater. Chem.*, **5**, 2165 (1995).
[6] P.G. Schouten, J.M. Warman, M.P. de Haas, C.F. van Nostrum, G.H. Gelinck, R.J.M. Nolte, M.J. Copyn, J.W. Zwikker, M.K. Engel, M. Hanack, Y.H. Chang, W.T. Ford. *J. Am. chem. Soc.*, **116**, 6880 (1994).
[7] P.G. Schouten, J.M. Warman, M.P. de Haas, J.F. van der Pol, J.W. Zwikker. *J. Am. chem. Soc.*, **114**, 9028 (1992).
[8] B. Blanzat, C. Bartou, N. Tercier, J.-J. André, J. Simon. *J. Am. chem. Soc.*, **109**, 6193 (1987).
[9] S. Chandrasekhar, B.K. Sadashiva, K.A. Suresh. *Pramana*, **9**, 471 (1997).
[10] S. Chandrasekhar. In *Advances in Liquid Crystals*, Vol. 5, Academic Press, New York (1982); *Mol. Cryst. liq. Cryst.*, **14**, 3 (1993).
[11] A.M. van de Craats, J.M. Warman, K. Müllen, Y. Geerts, J.D. Brand, *Adv. Mater*, **10**, 36 (1998).
[12] A.M. van de Craats, J.M. Warman, A. Fechtenkötter, J.D. Brand, M.A. Harbison, K. Müllen, *Adv. Mater*, **11**, 1469 (1999).
[13] H.-.T. Nguyen, C. Destrade, J. Malthête. *Adv. Mater.*, **9**, 375 (1997); *Handbook of Liquid Crystals II*, Vol. 2B, Chap. XII, D. Demus, J.W. Goodby, G.W. Gray, H.-W. Spiess, V. Vill (Eds), Wiley-VCH, (1998).
[14] J. Malthête, H.-T. Nguyen, C. Destrade. *Liq. Cryst*, **13**, 171 (1993).
[15] K.E. Rowe, D.W. Bruce. *J. Mater. Chem.*, **8**, 331 (1998).
[16] C. Alstermark, M. Eriksson, M. Nilsson. *Liq. Cryst.*, **8**, 75 (1990).
[17] D. Fazio, C. Donnio, Y. Galerne, D. Guillon, D.W. Bruce. *J. Mater. Chem.*, **11**, 2852 (2001).
[18] A.E.A. Contoret, A.J. Eastwood, S.R. Farrar, S.M. Kelly, J.E. Nicholls, M. O'Neill, G.J. Richards, C. Wu. *Mol. Cryst. liq. Cryst.*, **368**, 271 (2001).
[19] N.H. Sultana, S.M. Kelly, B. Mansoor, M. O'Neill. *Liq. Cryst.*, **34**, 1307 (2007).
[20] H. Meier, E. Prass, G. Zerban, F. Kosteyn. *Z. Naturforsch.*, **43b**, 889 (1988).
[21] B.P. Hoag, D.L. Gin. *Adv. Mater.*, **10**, 1546 (1988).
[22] C. Gadermaier, G. Lanzani, G. Cerullo, M. Zavelani-Rossi, U. Theissel, B.P. Hoag, G. Leising, S. De Selvestri, D.L. Gin, *Synth. Metals.*, **121**, 1323 (2001).
[23] J. Kido, H. Shionoya, K. Nagai. *Appl. Phys. Lett.*, **67**, 2281 (1994).
[24] B. Schulz, M. Bruma, L. Brehmer. *Adv. Mater.*, **9**, 601 (1997).
[25] D.D.C. Bradley, M. Grell. *Adv. Mater.*, **11**, 895 (1999).
[26] A. Bacher, P.G. Bentley, D.D.C. Bradley, L.K. Douglas, P. Glarvey, M. Grell, K.S. Whitehead, M. Turner. *Synth. Metals.*, **111–112**, 413 (2000).
[27] A.E.A. Contoret, S.R. Farrar, P.O. Jackson, L. May, M. O'Neill, J.E. Nicholls, S.M. Kelly, G.J. Richards. *Adv. Mater.*, **12**, 971 (2000).
[28] M. Jandke, D. Hanft, P. Strohriegel, K. Whitehead, M. Grell, D.D.C. Bradley. *Proc. SPIE*, **4105**, 338 (2001).

[29] P. Strohriegel, D. Hanft, M. Jandke, T. Pfeuffer. *Mater. Res. Soc. Symp. Proc.*, **709**, 31 (2002).
[30] I. McCulloch, W. Zhang, M. Heeney, C. Bailey, M. Giles, D. Graham, M. Shkunov, D. Sparrowe, S. Tierney. *J. Mater. Chem.*, **13**, 2436 (2003).
[31] M. O'Neill, S.M. Kelly. *Ekisho.*, **9**, 9 (2005).
[32] M.P. Aldred, A.E.A. Contoret, S.R. Farrar, S.M. Kelly, D. Mathieson, M. O'Neill, W.C. Tsoi, P. Vlachos. *Adv. Mater.*, **17**, 1368 (2005).
[33] M.P. Aldred, P. Vlachos, A.E.A. Contoret, S.R. Farrar, W.C. Tsoi, B. Mansoor, K.L. Woon, R. Hudson, M. O'Neill, S.M. Kelly. *J. Mater. Chem.*, **15**, 3208 (2005).
[34] A.E.A. Contoret, S.R. Farrar, M. O'Neill, G.J. Richards, M.P. Aldred, S.M. Kelly. *J. appl. Phys.*, **93**, 1465 (2003).
[35] M.P. Aldred, A.J. Eastwood, S.M. Kelly, P. Vlachos, B. Mansoor, M. O'Neill, W.C. Tsoi. *Chem. Mater.*, **16**, 4928 (2004).
[36] S.R. Farrar, A.E.A. Contoret, M. O'Neill, J.E. Nicholls, G.J. Richards, S.M. Kelly. *Phys. Rev. B.*, **66**, 125107 (2002).
[37] A.P. Grekov, O.P. Shvaika. *J. Gen. Chem. USSR. (Eng. Transl)*, **30**, 3763 (1960).
[38] S.N. Sawhney, P.K. Sharma, A. Gupta, G.B. Singh, S. Bahi. *Indian J. Chem. B.*, **32**, 1190 (1993).
[39] R.F. Heck, J.P. Nolly. *J. org. Chem.*, **37**, 2320 (1972).
[40] G. Wittig. *Pure appl. Chem.*, **9**, 245 (1964).
[41] W. Williamson. *Justus. Liebigs. Ann. Chem.*, **77**, 37 (1851).
[42] W.A. Herrman, C. Brossmeier, K. Ofele, C.P. Reisinger, T. Priermeier, M. Beller, H. Fischer. *Angew. Chem. Int. Ed.*, **24**, 1848 (1995).
[43] W.E. Parham, E.L. Anderson. *J. Am. Chem. Soc.*, **70**, 4187 (1948).
[44] B. Neises, W. Steglich. *Angew. Chem. Int. Ed.*, **17**, 522 (1978).
[45] N. Miyaura, T. Yanagi, A. Suzuki. *Synth. Commun.*, **11**, 513 (1981).
[46] A. Suzuki. *Pure appl. Chem.*, **66**, 213 (1994).
[47] A.E.A. Contoret, S.R. Farrar, M. O'Neill, J.E. Nicholls, G.J. Richards, S.M. Kelly, A.W. Hall. *Chem. Mater.*, **14**, 1477 (2002).
[48] N.B. Colthup. *J. opt. Soc. Amer.*, **40**, 397 (1950).